

---

# Advancing from Conceptual to Numerical Modeling: Reducing Uncertainty in the Data-Scarce Dili Intergranular Aquifer System, Timor-Leste

---

[Marçal Ximenes](#)\*, José M. M. Azevedo, [João A. M. S. Pratas](#), Fernando P. O. O. Figueiredo, [Hafids Galant Amirru](#)

Posted Date: 6 March 2026

doi: 10.20944/preprints202603.0579.v1

Keywords: quaternary aquifer; conceptual modelling; groundwater flow model; Dili City; Timor-Leste



Preprints.org is a free multidisciplinary platform providing preprint service that is dedicated to making early versions of research outputs permanently available and citable. Preprints posted at Preprints.org appear in Web of Science, Crossref, Google Scholar, Scilit, Europe PMC.

Copyright: This open access article is published under a [Creative Commons CC BY 4.0 license](#), which permit the free download, distribution, and reuse, provided that the author and preprint are cited in any reuse.

Disclaimer/Publisher's Note: The statements, opinions, and data contained in all publications are solely those of the individual author(s) and contributor(s) and not of MDPI and/or the editor(s). MDPI and/or the editor(s) disclaim responsibility for any injury to people or property resulting from any ideas, methods, instructions, or products referred to in the content.

Article

# Advancing from Conceptual to Numerical Modeling: Reducing Uncertainty in the Data-Scarce Dili Intergranular Aquifer System, Timor-Leste

Marçal Ximenes <sup>1,\*</sup>, José M. M. De Azevedo <sup>2</sup>, João A. M. S. Pratas <sup>3</sup>, Fernando. P. O. O. Figueiredo <sup>4</sup> and Hafids Galant Amirrul <sup>5</sup>

<sup>1</sup> Divisão de Hidrogeologia e Engenharia Geológica, Instituto de Geociências de Timor-Leste (IGTL), Dili, Timor-Leste

<sup>2</sup> Centro de Geociências da Universidade de Coimbra, University of Coimbra, Coimbra, Portugal

<sup>3</sup> CITEUC - Centro de Investigação da Terra e do Espaço; Dep. de Ciências da Terra-Polo II, 3030-790 Coimbra, University of Coimbra, Portugal

<sup>4</sup> Geosciences Center, Department of Earth Sciences, University of Coimbra, Coimbra Polo II, 3030-790 Coimbra, Portugal

<sup>5</sup> Geological Engineering, Gajah Mada University, Yogyakarta, Indonesia

\* Correspondence: marcal.x@gmail.com; Tel.: +670-7829-6504

## Abstract

Dili, the capital of Timor-Leste, is experiencing increasing freshwater demand driven by population and economic growth. It totally relies on groundwater from the Dili Intergranular Aquifer System for supply. There is very little conceptual understanding of the system and little-to-no monitoring data. Understanding the hydrostratigraphy, recharge and surface-groundwater interactions, groundwater levels and abstractions are essential for sustainable groundwater use and management. These are the aims of this study, and a numerical model was created with such purpose. The model included scenarios to assess how the aquifer could react to future increases in groundwater abstraction. Trial and error calibrated the steady-state model, and a comparison of simulated results with observed heads revealed good agreement (RMS <10%). Transient scenario simulations demonstrate that recharge (direct, river infiltration, and mountain-block processes) is a key component of the water balance and plays a critical role in aquifer sustainability under increasing groundwater abstraction. Aquifer storage is projected to decrease significantly by 2054, with the magnitude depending on the range of recharge and abstraction rates considered. The model improves conceptual hydrogeological knowledge of the basin, highlights future work needed, and provides a robust basis for sustainable groundwater management and water risk mitigation in Dili.

**Keywords:** quaternary aquifer; conceptual modelling; groundwater flow model; Dili City; Timor-Leste

## 1. Introduction

Groundwater is essential for the economic and social well-being of urban populations in developing countries [1,2]. The growing dependence on groundwater, coupled with diminishing resources, has prompted the exploration of effective scientific methods for groundwater investigation and management [3], which are needed to understand the changing and complex nature of groundwater and its impact on ecosystems and communities [4]. To learn more about local groundwater systems, to predict their future states and to manage them sustainably, it is important to understand their current status [3,5,6,7,8]. Such an endeavor requires, as a first step, a solid conceptual understanding of an aquifer system, that is, a detailed picture that describes the hydrogeological processes occurring within the system. It may include geological, geophysical,

hydrological, hydrogeochemical, and other details according to the specific context of the aquifer and the study objectives [9]. Comprehensive knowledge of local lithology is crucial to understanding the movement of water and its quality within an aquifer. Three-dimensional (3D) lithological modelling is typically used as a baseline in groundwater studies to assess the hydrogeological heterogeneity of the subsurface and define hydrostratigraphic units (HSUs) [10,11]. A hydrostratigraphic unit can be defined as a part of a body of rock/soil that forms a distinct hydrologic unit with respect to the flow of groundwater [12]. It was later redefined by [13] as "a body of rock/soil distinguished and characterized by its porosity and permeability." Such information is key for a solid hydrogeological conceptualization [10], especially in regions characterized by significant hydrogeological heterogeneity [10,114]. Usually, a conceptual model uses cross sections, fence diagrams, maps, and tables to show how HSUs are spread out, how groundwater flows, what processes are controlling recharge, and what the hydrogeological parameters estimates are [10].

An effective assessment of groundwater resources can greatly benefit from reliable and consistent groundwater simulations [7,14]. Realistic hydrogeological conceptual models are essential for designing numerical flow models [10,11,4,15]. Numerical groundwater modeling can be applied to many groundwater investigations, such as to better represent the hydrogeological system and refine the conceptual model, to understand the flow system, to study the recharge dynamics and rates, to assess the groundwater resources' potential, to test different groundwater management approaches, and to investigate future impacts on the hydrological system from changes to stress factors such as recharge and abstraction [16]. Numerical groundwater modeling is a way to simplify the ultra-complex reality of the hydrogeologic system of an area.

Dili, the capital of Timor-Leste, is experiencing increasing demand for freshwater due to both population and economic growth. The city is located on alluvial plains of loose sedimentary deposits, overlaying the Dili Sedimentary Basin, which contains highly productive aquifers that store enormous volumes of water and have facilitated the settlement of a large number of people [17]. The Dili population totally relies on the coastal Dili intergranular aquifer system (DIAS) for water supply, which, as such, is the object of this study. Many have studied groundwater in Dili City [17,18,19,20,21,22,23,24,25,26,27,28]. The studies conducted have contributed to this field. However, DIAS still significantly lacks hydrogeological knowledge, including robust recharge estimates and dynamics and a solid conceptual model encompassing a 3D lithological model to describe layered sediments and hydrogeological units.

Rapid urban growth and development in Dili have raised concerns about impacts on groundwater resources, and therefore a deeper understanding of how urbanization and increased groundwater extraction affect local water supplies is needed. Due to population growth and more economic activity, the use of groundwater in Dili is expected to rise significantly in the next few decades [22]. There is currently no proper groundwater management in the Dili basin [24], which will undoubtedly lead to sustainability problems related to water availability and quality, including seawater intrusion. The aquifers in the Dili Basin have good yields with 30 production wells calculated to have produced 10.6 million cubic meters (mcm) from January to October 2019, with most extraction in the western zone [17]. This estimate does not include thousands of existing private wells [17]. Further, collecting accurate data on water abstraction is challenging [8]. On the other hand, dropping water tables in some production wells have been reported [19]. Therefore, increased long-term withdrawal, without considering the aquifer behavior in response to recharge and pumping, will put DIAS at serious risk of degradation and compromise the ability to meet water needs. Despite some hydrogeological studies, including a simple modeling attempt, many questions remain about DIAS's conceptual model. This, in turn, means water managers and decision-makers have little information or guidance to work with in relation to sustainable pumping, drilling, and contamination risks. Section 2, Description of Study Area, provides a more detailed discussion of existing studies and remaining hydrological questions.

The only groundwater numerical model of DIAS to date, to the best of our knowledge, estimated the safe yield for Dili's groundwater to be around 0.28 m<sup>3</sup>/s [22]. The authors considered a

homogeneous aquifer (i.e., no different stratigraphic units) and homogeneous recharge across the basin. The lack of detailed data on sedimentary layers, recharge dynamics, and clarity regarding DIAS' conceptual hydrogeological model prevented the authors from developing a more complex model. Only 14 pumping wells were used, which further limited their ability to model the system realistically. Therefore, further research is needed to improve the conceptual and numerical modeling of DIAS. Understanding the timing and magnitude of changes in aquifer storage is critical to assessing groundwater availability in the DIAS and its sustainable use. As such, the aim of this study is to gain a greater understanding of the Dili basin's hydrogeology and predict future groundwater availability. This work is done by creating a numerical groundwater flow model that allows us to simplify the complexity of the local geological and hydrogeological contexts. Hydrogeologists, planners and regulators need a flexible, advanced tool to identify key areas and rates of groundwater recharge and discharge and predict groundwater dynamics—this is usually done through numerical groundwater flow models [29]. MODFLOW is the most common groundwater modeling code used globally [30], and as such was chosen for this modeling exercise. More specifically, the objectives of the study are (i) to understand which variables might impact the water balance more (e.g. recharge, evapotranspiration, hydraulic properties, abstraction rates and locations, and hydrostratigraphy); (ii) to predict changes to the water balance according to different scenarios of recharge and abstraction changes; and (iii) to propose future work, arising from the knowledge and uncertainties here gained, that allows for further inquiry into the hydrogeology of the system and more-informed management decisions. This paper does not include the strategies for sustainable groundwater management concepts, nor do we propose policies and regulations to protect groundwater resources; we will discuss these in a separate paper. No previous studies explain in detail the lithological conceptual model and numerical model of the groundwater flow system in the whole study area. Therefore, this study fills the major gaps by creating a thorough conceptual model of the DIAS and predicting the groundwater flow patterns according to present and future abstraction and recharge dynamics.

## 2. Description of study area

### 2.1. Geographical context

Dili has a population of 280 000, considering the administrative posts of Dom Aleixo, Nain Feto, and Cristo Rei [31]. The rapid growth has led to more groundwater needed to sustain daily life and economic activities. This research focused on the alluvial aquifers of the Dili Basin, also known as DIAS, which is bounded by the sea to the north and limited by mountainous areas to the south (Figure 1). The study area is mostly flat, covering around 26 km<sup>2</sup>, with elevations between 1 and 63 meters above sea level. It is highly urbanized, mostly covered by residential, office, and commercial buildings. Topography inclines from south to north with a slope gradient of 0.5-6%, which can be > 6% around the foot of the mountains in the southern area [25]. The aquifers are recharged by rainfall and river infiltration [19,21,25] and most likely also mountain-block recharge from the southern hills. The region's hot tropical climate is heavily influenced by the West by West Pacific Monsoon and its mountainous topography. The wet season takes place between December and May and the dry season between June and November [32]. The mean annual precipitation is 994 to 1223 mm/year [25]. The mean temperature is around 27°C in coastal areas and around 22°C in the highlands [19].



current rivers, which comprise both floodplain and terrace alluvial deposits. In contrast, the coastal and central regions consist of marine sediments at specific depths and fluvial sediments exclusively in the upper layer, as documented by various drilling logs [17]. Due to limited data, the thickness of the basin is unknown, but some drilling reports indicate it may be more than 150 meters thick in the central area and gradually thin toward the south. The water level is shallower along the northern coast and deeper around the southern area, making it more vulnerable to seawater intrusion and bacteriological and chemical contamination in the northern zone [23]. Since the city lacks an urban plan and groundwater policy, groundwater quality is threatened by uncontrolled domestic wastewater and solid waste, as indicated by the presence of bacteria and nitrates [23]. Some wells have also been found to contain elevated levels of calcium, magnesium, and heavy metals [25].

**Table 1.** Summary of the previous DIAS' hydrogeological studies

Title	Method	Finding
Aquifer characterization in Timor-Leste using Ground Electromagnetics [18]	1. TDEM soundings at 35 locations	1. Dili Aquifer System comprises unconsolidated sands and gravels, with a shallow water table.
	2. Field Data Collection – Using 100m x 100m transmitter loops, measuring conductivity changes at different depths.	2. Recharge mainly occurs through monsoonal rains and river flow.
	3. Data Processing and Inversion – Generating conductivity-depth profiles to infer aquifer properties.	3. Saltwater intrusion is a concern, especially near the coast.
	4. Hydrogeological Interpretation – Integrating TDEM results with borehole data to assess aquifer depth, permeability, and water quality risks.	
Vulnerability assessment of climate change impacts on groundwater resources in Timor-Leste [19]	Acquisition and/or analysis of:	1. Dili is formed by intergranular aquifer and Aileu Fractured Rock Aquifer (southern part of Dili). Localized fractured aquifers (e.g., in Aileu) are less affected by sea level rise but are highly sensitive to changes in rainfall.
	1. Geological data	Groundwater levels are declining due to over-extraction.
	2. Climate data	2. Saltwater intrusion is increasing, particularly in wells near the coastline.
	3. Drilling data	3. The aquifer is highly vulnerable to both climate change and urbanization.
	4. Water chemistry	4. Nitrate is higher (> 5 mg/l) around the central part of Dili. The major chemical elements analyses indicated the ionic composition of the groundwater is very closely related to the source rock material of the sediments.

Title	Method	Finding
	Acquisition and/or analysis of:	1. Urbanization and land cover change: Rapid, unplanned urban development, including the conversion of wetlands and agricultural land, has reduced natural groundwater recharge and increased extraction.
	1. Drilling data (pumping data)	2. Tourism growth: Tourist arrivals surged from 14,000 in 2006 to 51,000 in 2011, further increasing groundwater demand in hotels and commercial facilities.
	2. Monitoring well data	43. Limited surface water resources: Inadequate surface water availability has intensified reliance on groundwater.
Groundwater Environment in Dili, Timor-Leste [20]	3. Groundwater use data	4. Declining groundwater quantity: At the Comoro Wellfield, groundwater levels fell by 6.0 m between 2008 and 2013, with production capacity of key wells decreasing by up to 75,000 m <sup>3</sup> /year.
	4. Census data	6. Groundwater quality issues: Elevated TDS, iron, nitrate, and turbidity were detected in several wells, while microbiological contamination (coliform bacteria) was found in 70% of tested sources.
	1. Analytic Hierarchy Process (AHP) for Weighting Factors	6. Management implications: The study emphasizes the urgent need for improved groundwater management strategies, regulatory reforms, and investment in alternative water sources to ensure a sustainable water supply for Dili's growing population.
Delineation of groundwater potential zones in the Comoro watershed, Timor Leste using GIS, remote sensing and analytic hierarchy process (AHP) technique [21]	2. GIS-Based Weighted Overlay Analysis	1. GIS, remote sensing, and AHP successfully identified groundwater potential zones in the Comoro watershed.
		2. 13.5 km <sup>2</sup> (5.4%) of the Comoro catchment area has very high groundwater potential, mainly in northwestern alluvial plains.
		3. 87.8% of the area has poor to very poor groundwater potential, mostly in the southern and central regions.
		4. Validation with bore well data confirms the reliability of the delineated zones.
		5. The results provide a scientific basis for groundwater exploration, management, and policy-making in Timor-Leste.

Title	Method	Finding
Assessment of groundwater yield of Dili Aquifer, Timor-Leste [22]	Acquisition and/or analysis of:	1. Groundwater flow: Controlled primarily by topography.
	1. Climate data	2. Safe yield: The study estimates a maximum abstraction rate of 0.28 m <sup>3</sup> /s, which balances recharge without depleting storage, corresponding to a groundwater level of 7.8 m below ground level (mbgl).
	2. Groundwater level data from piezometers and pumping wells	3. Sustainable yield: To ensure long-term sustainability, abstraction should range between 0.23–0.28 m <sup>3</sup> /s, maintaining the critical water level.
	3. Groundwater modelling using MODFLOW	4. Future risks: Increased groundwater extraction and reduced recharge due to urbanization may stress the aquifer, leading to over-extraction and potential saltwater intrusion.
Initial observations of water quality indicators in the unconfined shallow aquifer in Dili City, Timor-Leste: Suggestions for its management [23]	1. Physicochemical and Microbiological data	1. Dili's unconfined aquifer is heavily contaminated, especially in densely populated areas with poor sanitation.
	2. GIS and kriging techniques to map contamination zones.	2. The quality of groundwater is deteriorating due to microbiological pollution, and other chemical contaminants.
		3. Shallow wells are the most vulnerable, especially in low-gradient and swampy areas.
Groundwater Resources Development Project for the Water Supply of Dili Metropolitan Area [17]	1. Groundwater well inspections.	1. The Dili Aquifer System consists of:
	2. Resistivity surveys to determine aquifer characteristics.	o Shallow aquifers (5–20m deep) with moderate recharge.
		o Deep confined aquifers (up to 100m), which are less vulnerable to contamination.
		2. The total estimated groundwater recharge is 2.9 million cubic meters per year (MCM/year), based on simple water balance method.
	3. Environmental and social impact assessments.	3. The Comoro River plays a major role in groundwater recharge, but high extraction rates are exceeding sustainable limits. 4. Current groundwater extraction is ~37,700 m <sup>3</sup> /day, but demand is expected to increase to 71,000 m <sup>3</sup> /day by 2036. 5. More than 70% of produced water is lost due to leaks in the distribution system.

Title	Method	Finding
<p>Identification of hydrochemical processes and assessment of groundwater quality: a case study of the intergranular aquifer in Dili City, Timor-Leste [25]</p>	<p>1. Water quality index (WQI)</p> <p>2. Geographic information system (GIS) for spatial analyses of contamination distribution</p> <p>3. Statistical methods (principal component analysis and hierarchical cluster analysis) to determine the group of water types and trace chemical origins.</p>	<p>6. Groundwater over-extraction is leading to declining water levels and risk of saltwater intrusion in coastal areas.</p> <p>1. The tests revealed that the levels of EC, Ca, Mg, F, Fe, Al, As, Zn, Pb, and Mn in some wells were higher than WHO (2011) recommendations.</p> <p>2. The dissolution of silicate minerals like feldspar, muscovite, and biotite in the bedrock, as well as carbonate minerals, are the main factors that change the chemistry of groundwater in the study area.</p> <p>3. The spatial distribution of groundwater quality describes that poor water quality is observed in the southern part of the study area, which reveals the dissolution of silicate minerals in the aquifers.</p>
<p>Evaluating the concentration, distribution, and contamination of toxic metals in the urban soil of Dili, Timor-Leste [26]</p>	<p>Acquisition and/or analysis of:</p> <ul style="list-style-type: none"> <li>• Pollution index: Enrichment Factor (EF), Geo accumulation Index (Igeo), The contamination factor (CF) and pollution load index (PLI),</li> <li>• Potential ecological risk index</li> <li>• Statistical analyses (principal component analysis and hierarchical cluster analysis) to trace contamination sources.</li> </ul>	<p>1. Spatial distribution maps showed that metal contaminants were unevenly distributed, especially near residential, commercial, and airport areas.</p> <p>2. PCA revealed three components accounting for 71% of the total variance, linking Cd, Cu, Cr, Ni, Zn, As, Fe, Mn, and Pb to different sources. HCA grouped the metals into clusters, showing that most are of human origin, while iron (Fe), cobalt (Co), and arsenic (As) are from natural sources.</p> <p>3. The Pollution Load Index and Ecological Risk Index indicated moderate risks from cadmium (Cd) and lead (Pb), while the threats posed by other metals were lower.</p>
<p>Geology of The Lower Comoro Fluvio-Deltaic Accumulation: Outcrop, Resistivity, Drilling Data And Their Implications For Groundwater Resources [27]</p>	<ul style="list-style-type: none"> <li>• Outcrop analysis – 10 outcrop sections were logged and classified into lithofacies.</li> <li>• Borehole database – over 4,373 wells compiled, with detailed lithology from 52 reliable wells.</li> </ul>	<p>1. Facies Associations (six types): Channel fill (FAcb1), Major channel bar (FAcb2), Major distributary channel (FAcb3), Minor distributary channel (FAcb4), Floodplain (FAfp), Marine-influenced deposits (FA-mbd).</p> <p>2. Groundwater Implications: Good aquifers: Channel fill (FAcb1), major distributary channel (FAcb3), minor distributary channel (FAcb4). Variable role: Marine-influenced deposits (FA-mbd) can function both as aquifer and aquitard. Poor aquifers/aquitards: Major channel bars (FAcb2) and floodplain deposits (FAfp).</p>

Title	Method	Finding
	<ul style="list-style-type: none"> <li>• Geophysical surveys – six electrical soundings (ES) and 35 electrical resistivity tomography (ERT) profiles to image subsurface stratigraphy.</li> </ul>	3. Spatial implications: The central Comoro River zone represents the most favorable groundwater reservoir, while the eastern and western LCFDA are less favorable due to poorly sorted sediments and smaller rivers.
	<ul style="list-style-type: none"> <li>• Integration – cross-sections and depositional models built by correlating drilling, resistivity, and surface geology.</li> </ul>	
Assessment of Groundwater Vulnerability in Dili City, Timor-Leste using an Improved DRASTIC and Analytic Hierarchy Process (AHP) Method: Implications for Wastewater Management [28]	<p>Analysis of contamination vulnerability through:</p> <ol style="list-style-type: none"> <li>1. GIS model based on (a) DRASTIC, (b) modified DRASTIC, and (c) modified DRASTIC-AHP3.</li> <li>2. Bacteria (T. Coliform from some wells) to validate to model</li> </ol>	<ol style="list-style-type: none"> <li>1. Model performance: The Modified DRASTIC-AHP model showed higher accuracy than the other models, with <math>R=0.59R = 0.59R=0.59</math>, and classified groundwater vulnerability into four categories: 15.8% very low, 34.7% low, 32% moderate, and 17.5% high.</li> <li>2. Spatial patterns: The model indicated the highest vulnerability in the central-to-northern part of Dili City, while the southern part exhibited the lowest vulnerability scores.</li> <li>3. Sensitivity analysis: Recharge, aquifer media, and hydraulic conductivity were identified as the main influencing factors.</li> </ol>

The Comoro watershed has by far the largest catchment area, enhancing the infiltration potential due to larger volumes flowing through in this western part of DIAS. The results of pumping tests confirm this area's high permeability. The groundwater pumping rate through production wells is  $>10$  l/s, while the pumping around the central to eastern area is  $<10$  l/s, as observed in the field. The relatively homogeneous coarse sediment materials in the Western area reflected a good aquifer potential from groundwater exploitation [17,20,2123,25], but less of the confining bed may also allow for groundwater contamination and seawater intrusion risk. Groundwater abstraction reduces storage and baseflow, which in turn reduces streamflow and impacts low environmental flows during dry periods [35], which is a risk around the Comoro River. In addition, several boreholes also report that groundwater quality (electrical conductivity value could be  $>1500$   $\mu\text{S}/\text{cm}$ ) becomes poor when drilling reaches depths  $> 55$  m around the North to Central Zone.

Groundwater recharge results from direct infiltration of precipitation and river infiltration resulting from runoff from the high mountains in the southern area [17,20,2125]. Additionally, it is likely that mountain-block recharge occurs in the interface of the Southern mountains with the Dili sedimentary basin, especially in the Comoro catchment because of its larger area. The connection between groundwater and rivers is complex because of the multi-layered flow nature of DIAS, the dry-wet season patterns system of Dili. Typically, the Comoro River flows continuously during the wet season and remains dry during the dry season. It is possible, however, to observe a small wetland with abundant water at the mouth of the Comoro River during the dry season, just above sea level, which is most likely an expression of the groundwater table, representing fresh water sitting on top of the seawater. The data indicates that the water table close to the coast remains reasonably constant, which is because of the constant hydraulic head at the coastline. All other rivers typically run because of rain events and are dry otherwise.

Inadequate regulation of groundwater extraction leads to the uncontrolled operation of many unreported wells. Many private and domestic wells operate without meters, causing an underestimation of actual withdrawals. In 2021, Comoro had 4,373 wells as identified [36]. In the central and eastern zones there were fewer wells, probably because of geological conditions that are less favorable for drilling and/or water quality, although there is no comprehensive well register for those areas. There is no updated information on this matter.

### 3. Materials and Methods

The methodology for this study includes, firstly, a combination of several data sets to create a lithological model, which is followed by the hydrogeological conceptual model. Secondly, a steady-state groundwater flow model is set up and calibrated, which includes estimations of groundwater recharge, sensitivity analysis of hydraulic parameters and other water-balance variables, and definition of boundary conditions. Analyses of model results assisted in refining the conceptual model. Thirdly, future possible scenarios of abstraction and recharge are tested through a transient groundwater numerical model, which helps understand how DIAS will respond to changes in hydrological stresses over the next 30 years.

#### 3.1. Conceptual model development

##### 3.1.1. Data Source

Hydrogeologists use surface and subsurface data to reconstruct these systems to enhance their understanding of hydrogeological systems and improve quantitative modelling [37]. The borehole database created for this work includes information such as elevations, details of sediment layers, and water levels, which was collected from local drilling companies (e.g., H2O Pty. Ltd. 2007–2018; Mira Mar Unip. Ltd. 2014–2023; Geotechnic Pty. Ltd. 2019–2022); spatial geological data (including shapefiles) from the Instituto do Petroleo e Geologia (IPG) database (2014); and the Government of Timor-Leste (2020). Additional groundwater depth data was obtained from: (i) IGTL's database, which was then combined with field data collected for this study (2018–2023); (ii) the Government of Timor-Leste (2020); and (iii) four piezometer monitoring data from 2020–2021, obtained from the National Directorate for Water and Sanitation Regulations (ANAS/DNRAS, 2021). These data were combined with a 5-meter resolution LIDAR digital elevation model (DEM) obtained from the IGTL database and used to determine the DIAS water table elevation.

##### 3.1.2. Lithostratigraphic model of DIAS

In this study, individual borehole coordinates, elevations, and hydrostratigraphic unit intervals derived from borehole lithological logs were added to the Leapfrog Geo software (Figure 2). This is a commonly used, user-friendly application for three-dimensional modeling of subsurface geology and hydrostratigraphy, surface, and subsurface data while interpolating borehole data to construct a three-dimensional spatial model [38]. The conceptual model for the DIAS is based on the surface elevation DEM. Lithological data from 157 borehole logs, including information gathered from field investigations, were used to conceptualize the sedimentary deposits into six strata and to subdivide the hydrostratigraphy into a two-unit hydrostratigraphy (Figure 7-b) with respect to the study area boundary. Delineation of these units divides the sedimentary layer into zones of different hydraulic properties and geometries. This division allows for a more comprehensive mapping and understanding of the groundwater flow system [39].

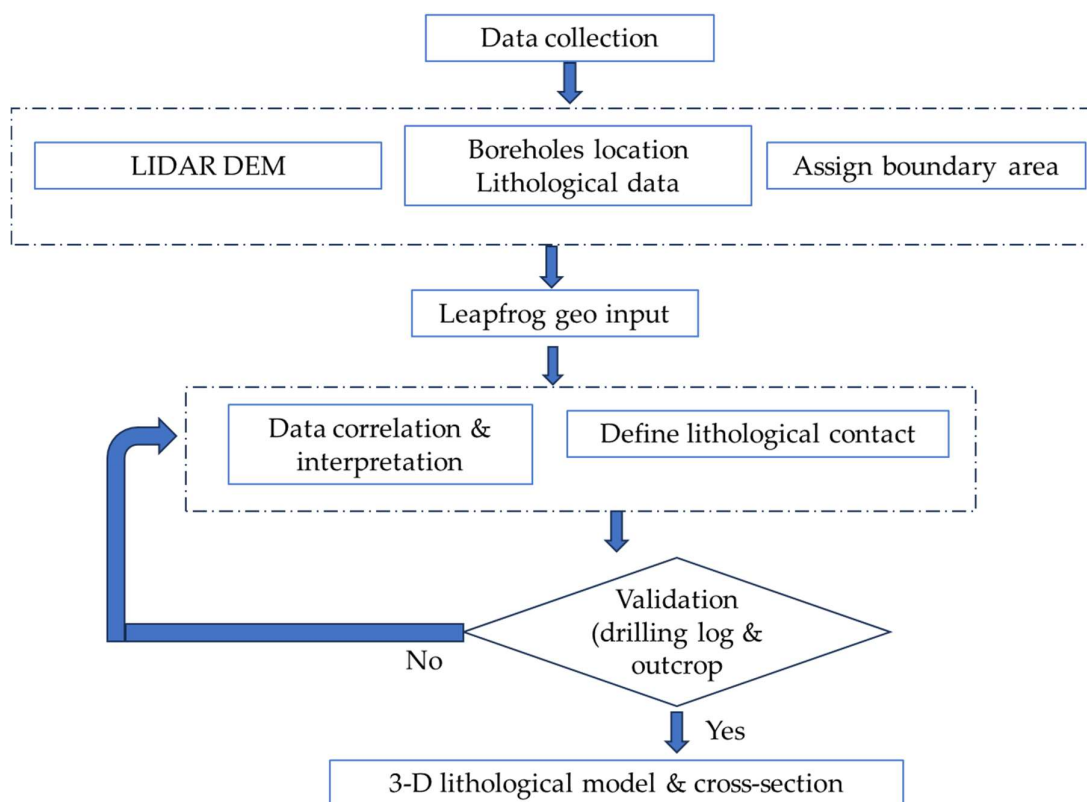


**Figure 2.** Flowchart showing the development of the lithological model.

### 3.1.3. Hydrogeological Conceptual Model of DIAS

The conceptualization is a necessary simplification of the natural system, as it is not feasible to incorporate all of its complexities into a computer model [40]. Lithostratigraphic models help make more realistic hydrogeological conceptual models that summarize the hydrogeological knowledge of the modeled site, giving a framework for designing numerical models [10]. Usually, a conceptual model uses cross sections, fence diagrams, and tables to show HSUs' architecture, maps of groundwater heads and flow directions, analysis of recharge/discharge dynamics and rates, and estimates of hydrogeological parameters [10].

The conceptual modeling of DIAS includes lithostratigraphic modeling, understanding surface-groundwater interactions, recharge dynamics, and the analysis of groundwater levels and flow directions. This procedure, in turn, allowed the selection of appropriate boundary conditions for the numerical model. Crucially, the numerical modeling calibration process allowed for refinement of the conceptual model. This was done by analyzing the performance of the model against measured water levels according to different conceptual understandings of recharge rates and processes. This approach is in close alignment with modeling best practices suggested by [41]: "There should be an ongoing process of refinement and feedback between conceptualization, model design, and model calibration such that revisions and refinements to the conceptual model can be made over time."

### 3.2. Steady-state numerical groundwater modeling using visual MODFLOW

Visual MODFLOW Flex was employed to simulate groundwater flow [42]. MODFLOW simulates groundwater dynamics within the aquifer by accounting for confined and unconfined conditions, using the finite difference method and a block-centered approach. It incorporates multiple recharge and discharge sources, such as recharge, groundwater extraction by wells, runoff from precipitation, flow to/from riverbeds and sea, and spring flow [43]. It can simulate multiple or single aquifer layers, accommodate various boundary conditions and anticipate future aquifer

conditions using different pumping and climate scenarios [44]. Many studies have successfully applied combinations of GIS and MODFLOW to develop conceptual models and groundwater flow models in their study areas [10, 16, 30,28,5]. MODFLOW can be a flexible and powerful tool for simulating groundwater flow in a range of subsurface environments, from simple to complex [45].

### 3.2.1. Model setup and assumptions

The hydrostratigraphic and conceptual models were used as the basis for the steady-state groundwater flow model. The study area was discretized by dividing it into 125 rows and 250 columns. Thus, the total number of cells over the area is 31,250, with each cell measuring 45 m x 45 m in each layer. The dominant topographic slope of the area determined the main regional flow direction, which guided the orientation of the grid.

The following assumptions were made for the modeling:

1. The river partially penetrates the aquifer system and has vertical banks;
2. The river is not separated from the aquifer by any confining material;
3. The influx into the system is primarily through recharge due to rainfall;
4. Naturally, rivers interact with groundwater through river leakage. The phenomenon occurs in two forms: inflow (positive leakage), where water flows from the river to the aquifer, and outflow (negative leakage), where water flows from the aquifer to the river;
5. The flow in the aquifer system is in steady state;
6. Each lithological unit is homogeneous and isotropic;
7. The groundwater system is assumed to be a porous medium, which has homogeneous and isotropic properties in the horizontal direction ( $K_x = K_y$ );
8. The horizontal hydraulic conductivity value is assumed to be 1 order of magnitude greater than the vertical hydraulic conductivity value ( $K_x=K_y=10K_z$ );
9. The southern hilly part and the basement, in the form of metamorphic rock, are assumed to be an impermeable layer and are therefore made inactive cells in the model;
10. The model was calibrated for the period 2008–2023, using drilling and pumping data (2008–2022), recharge and evapotranspiration data (2021–2023), and river conductance and boundary condition data. Other hydrogeological parameters, including vertical hydraulic conductivity, specific yield, and specific storage, were assigned based on reference values from the literature [46,47,48], due to the absence of local field measurements.

Visual MODFLOW Flex imports data in ASCII or Surfer (.grd) formats [49]. In this study, surface elevation, layer elevation, and groundwater level data were formatted as Surfer (.grd) files and used as model inputs. [49]. The shape file layers or input parameters necessary for simulating groundwater flow in Visual MODFLOW Flex include (1) active and inactive cells, (2) elevations of the top and bottom of each layer, (3) horizontal and vertical hydraulic conductivity, (4) recharge rate, and (5) initial hydraulic heads.

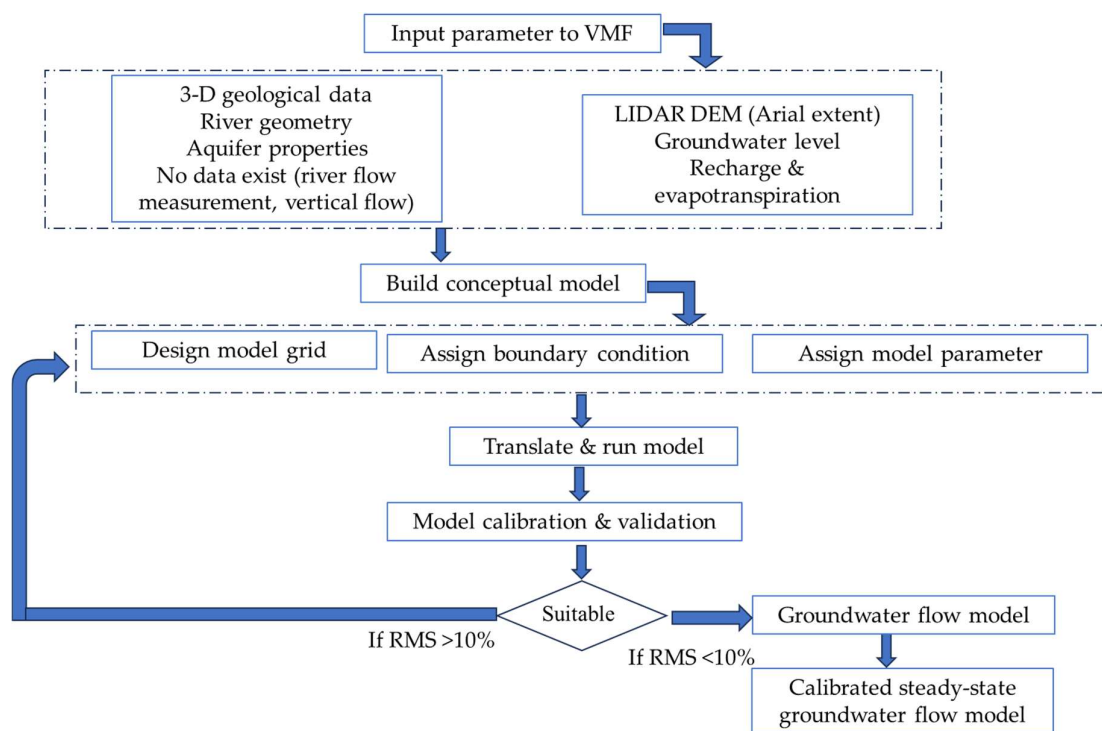


**Figure 3.** Flowchart showing the development of the lithological model

### 2.2.2. Aquifer hydraulic parameters

Aquifer parameters, such as hydraulic conductivity ( $K$ ), specific storage ( $S_s$ ), and specific yield ( $S_y$ ), govern groundwater flow [50]. Based on the lithological description and limited aquifer test data, the domain was divided into six units, each with a different  $K$ . Alluvial sediments typically exhibit significant heterogeneity, with  $K$  values varying across various orders of magnitude [51]. Since there are limited aquifer properties data for the area from pumping tests, we use the existent local data in combination with reference for  $K$  [47] (Table 2). As for the other hydraulic properties, namely  $S_s$  and  $S_y$ , we used MODFLOW default values in the absence of any accurate local data. The initial  $K$  values were modified within appropriate ranges during steady-state calibration to obtain best-fit models. Initially, the model used a single  $K$  value for both clay layers. However, after calibration, it became necessary to adjust these values separately to better reflect field conditions observed in some wells. Field conditions indicate that the upper clay layer consists of sandy clay, while the lower layer is made up of pure clay. Due to their differing properties, separate  $K$  values were assigned to each layer. The initial and calibrated parameters in the study area are presented in Table 2.

**Table 2.** Initial and calculated hydraulic properties of DIAS.

Initial value	Kx (m/s)	Ky (m/s)	Kz (m/s)	Data Source
Hydrostratigraphic unit-1				
Sand 1	8.50E-03	8.50E-03	8.50E-04	Pumping test
Clay 1	2.00E-06	2.00E-06	2.00E-07	Domenico and Schwartz, (1990)
Sand 2	2.80E-03	2.80E-03	2.80E-04	Pumping test
Clay 2	3.50E-07	3.50E-07	3.50E-08	Domenico and Schwartz, (1990)
Sand 3	4.50E-04	4.50E-04	4.50E-05	Pumping test

Initial value	Kx (m/s)	Ky (m/s)	Kz (m/s)	Data Source
Hydrostratigraphic unit-2				
Bedrock	2.06E-10	2.00E-10	2.00E-11	Domenico and Schwartz, (1990)
After calibration				
Sand 1	2.60E-05	2.60E-05		2.60E-06
Clay 1	2.80E-06	2.80E-06		2.80E-07
Sand 2	2.80E-03	2.80E-03		2.80E-04
Clay 2	3.50E-08	3.50E-08		3.50E-09
Sand 3	5.71E-06	5.71E-06		5.71E-07
Hydrostratigraphic unit-2				
Bedrock	4.50E-10	4.50E-10		4.50E-11

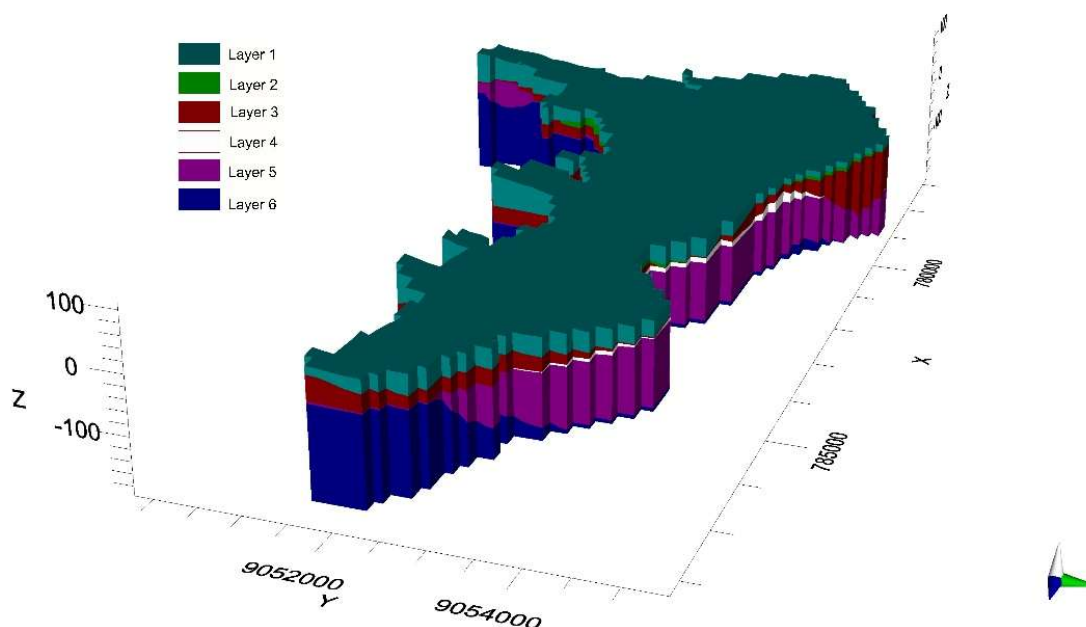


**Figure 4.** Spatial distribution of the lithostratigraphic units, each corresponding to calibrated horizontal hydraulic conductivities for the groundwater flow model.

### 3.2.3. Groundwater Recharge

Groundwater in storage has a changing value that fluctuates in response to seasonal and long-term changes in recharge and discharge rates to and from the aquifer. Recharge is usually defined as the water from precipitation and surface-water bodies that infiltrates deep enough below the ground surface to reach the water table, where it joins the groundwater zone [52,53]. Recharge cannot be directly measured [54,55], and it is difficult to be estimated with a high degree of certainty [56]. In the absence of data that allow us for more comprehensive recharge calculations, the empirical recharge estimate methods (Equations 1-4) were also used to estimate how groundwater recharge is distributed. Since DIAS has different spatial hydrological conditions (Figure 1), it is relevant to input the recharge rate of each zone. The quantification of recharge in the study area was done using the

simple water balance equation, where recharge ( $R$ ) is equal to precipitation ( $P$ ) minus real evapotranspiration ( $E_{Tr}$ ) minus run off ( $R_o$ ).  $E_{Tr}$  was calculated by applying Turc model [57].

Surface runoff was calculated by applying the empirical runoff equation from the Department of Agriculture of India (1990), which has been shown to be suitable for the island of Java (Institute Teknologi Bandung, 2001) and has been used in various Indonesian studies [58,59] for Jogjakarta and Sumbawa, Indonesia. DIAS is consistent with the Indonesian geographical context; thus, this method is considered adequate to be applied for our case study.

DIAS is recharged by rainfall and river infiltration [16,18,22], and most likely also mountain-block recharge from the southern hills. River infiltration and mountain block are processes particularly relevant for the Comoro River, which has a large, mountainous 207.29 km<sup>2</sup> basin. Typically, mountain blocks recharge constantly and slowly, bringing groundwater into the aquifers at the interface between the mountain and the edge of the sedimentary basin. Additionally, recharge at the mountain front is also likely to play a role in the overall recharge process, which takes place through the infiltration of water from streams located at the mountain front. It is likely that groundwater is directly subject to evapotranspiration when it is very shallow, which happens close to the coastline and riverbeds (especially the Comoro River). The DIAS area was divided into three main recharge zones: west, central, and east, based on the distribution of monitoring stations and the river catchments of each area (Figure 1). As such, the recharge calculations as per Equations 1–4 were performed for each of those areas, which only represent direct rainfall recharge.

As there is no data available to calculate these additional sources of recharge (i.e. river infiltration, and mountain block and front processes), we opted for calculating recharge for the upper Comoro catchment using the same methods as above and adding that recharge to zone one (as zone one is the end of the Comoro catchment). We assume the same recharge rate in mm/year over zone one, which in turn means a reduction in total volume recharge of 88% because of the small area compared to the total upstream area. This might be a gross simplification and limitation for recharge calculations, but in the absence of any data that can allow for more accurate estimations, it is a reasonable approach. Future studies should refine recharge calculations based on target fieldwork and new datasets.

For the DIAS direct recharge calculations, three years of rainfall data (2021–2023) from five stations (Table 6) were obtained from DNRAS, the National Directorate of Meteorology and Geophysics (DNMG) and IGTL. Temperature data were sourced from DNMG records (focusing on the flat area). However, due to limited climate data for the same period in the upstream Comoro basin, rainfall records from 2012 to 2019 were used [17]. We acknowledge these data sets are very limited, but the data availability in Timor-Leste is a major limiting factor for hydrogeological work, and our analysis is the best that can be done with available information in a timely manner to model the aquifer.

#### 3.2.4. Boundary conditions and initial conditions

To describe how water enters or leaves the simulated aquifer system, it is important to consider the boundary and initial conditions, the elevation of the top and bottom layers, the recharge rate,  $K$ , the abstraction of groundwater from wells, rivers and bodies of seawater. These factors were used to run the flow model. The next step was to construct the model, primarily by converting the conceptual model into input files for the numerical model. Finally, calibration was carried out to demonstrate that the model could produce field-measured heads and flows, which were then used as calibration values.

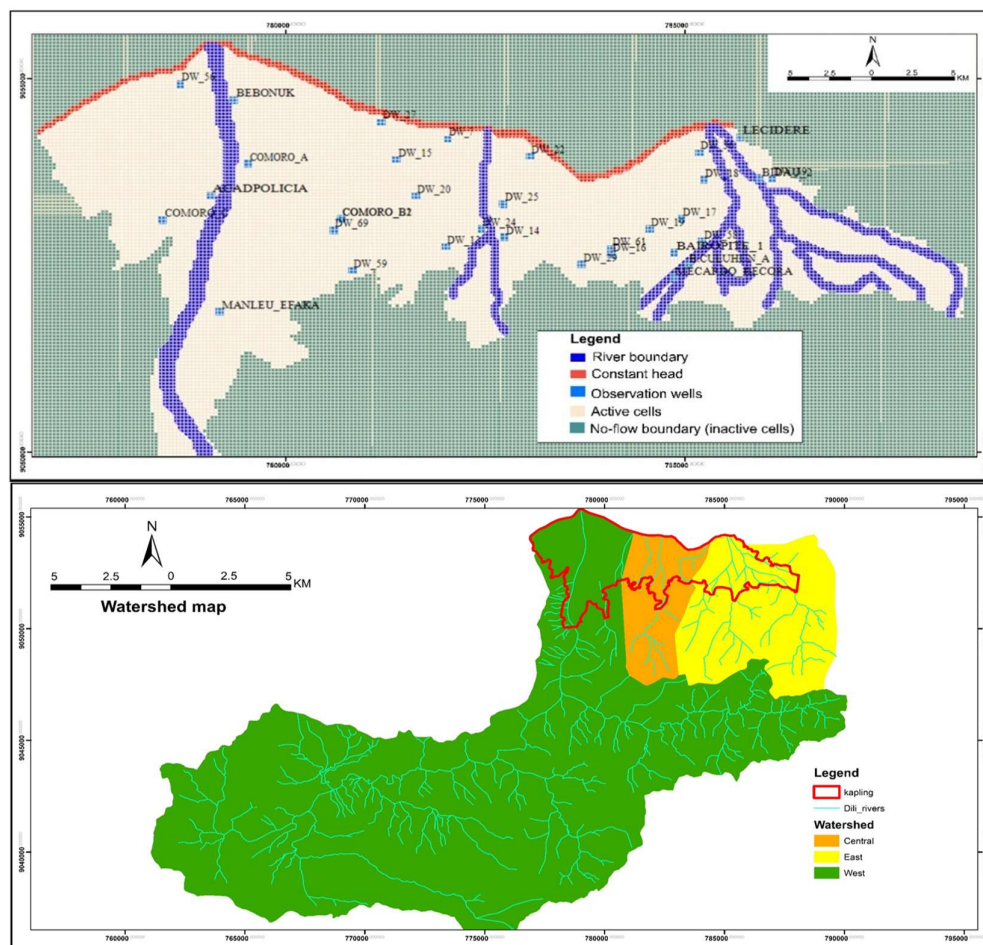


**Figure 5.** (a) Map showing grid pattern: active cells, inactive cells, and boundary conditions, (b) Map of watershed boundary of each zone.

The following boundary assumptions were made for the modeling:

- No-flow boundary: The model base is assigned to a zero-flow boundary, as the bedrock underlying the principal aquifer is poorly permeable. The no-flow boundary was assigned in the hilly region as an inactive cell located in the southern part of the study area, which contains metamorphic rocks; therefore, the western, eastern, and southern boundaries are not included in the model;
11. Constant head boundary (CHB): The constant head boundary in this model is used to represent boundary conditions that have a fixed head and do not change with time. In this model, the constant head boundary is used to represent the coastline, so the constant head boundary is used to simulate groundwater discharge to and from the sea;
  12. River: The river boundary conditions represent the Comoro, Maloa, Lahene, Taibesi/Kuluhun, and Becora/Bidau rivers, which generally flow from south to north. All rivers are dry during the dry season and flow only during the rainy season. In the dry season, the Comoro River retains water only in its upstream section, while the downstream section is dry, indicating it is a losing stream. This suggests that surface water from the Comoro River infiltrates into the aquifer, contributing to groundwater recharge. The general parameters of the river boundary conditions are given in Table 3.

**Table 3.** River boundary conditions.

No	Rivers name	River stage (m)	Riverbed bottom (m asl)	River width (m)	Riverbed thickness (m)
1	Comoro	77-0.7	69.5-0.34	104-142	2-3
2	Maloa	44-1.5	42-0.9	10-24	2-2.5
3	Lahane	43.8-1.5	40.78-0.6	14-25	1.5-2.5
4	Taibesi	56.3-13.5	53.3-8.5	1-20	2-2.5
5	Becora	63.8-11.4	58.8-6.4	7-10	2-3

In the river package of MODFLOW, river boundary conditions are used to represent natural boundaries like rivers in the Dili area. Groundwater level data from monitoring wells helped establish the initial head and served as calibration data for the steady-state model.

Regarding the governing equation for analyzing the river boundary condition, we follow the MODFLOW manual classic river package or the MODFLOW-6 gwf-riv package. The river package requires river stages, riverbed elevation, river conductance, and aquifer head. We considered river stages, bed elevation, and conductance in three segments for each of the four selected rivers. In the absence of field data, the initial conductance of the riverbed was set up as default from MODFLOW and was adjusted during the calibration period.

### 3.2.5. Modelling

MODFLOW is a modular three-dimensional finite difference groundwater modelling code [60]. In it, the developed conceptual model is converted into a mathematical model that simulates groundwater flow indirectly by means of a governing equation thought to represent the physical processes that occur in the system, together with equations that describe heads or flows along the boundaries of the model [61]. The equation representing the transient flow of a compressible fluid in a non-homogeneous anisotropic aquifer is derived by integrating Darcy's law with the continuity equation. Groundwater modelling was applied using the equation for three-dimensional groundwater flow [48,60].

### 3.2.6. Steady state calibrations

In the absence of pre-development data, or any other meaningful dataset, the steady-state groundwater flow model has been constructed by using the water level of September to November 2021 and calibrated to represent the natural flow system, where it represents a natural balance regime of inputs and outputs from the aquifer system. The calibration involved matching the observed heads in the aquifer with the hydraulic heads simulated by Visual MODFLOW. Three years of measured water level data from monitoring wells combined with initial water level data from domestic wells within the model area were used for calibration, with hydraulic conductivities and local recharge rates as calibration variables.

To date, just four monitoring wells have been installed on the north coast and in the western part of Dili in recent years [17,22], but they do not cover the central and eastern areas. We selected DM1, DM3 and Kuluhun-A and then combined it with water level data from 30 households for steady-state calibration, with the hydraulic values used for the model heads, with the observed heads representing the natural groundwater piezometric surface.

A series of model runs were carried out to match the observed and simulated water level contours by varying the  $K$  values and boundary conditions. The calibration parameters were modified until a satisfactory match between simulated and observed hydraulic heads, considering a root mean square error (RMS) < 10%, and baseflow values was achieved to better represent the actual conditions.

### 3.2.7. Sensitivity analysis

Sensitivity analysis is a critical component of modeling studies due to the uncertainties associated with estimating aquifer parameters, stresses, data availability and boundary conditions. The aim is to assess the impact of different model parameters and hydrological stresses on the aquifer system and to identify the most sensitive parameters that require focused investigation in subsequent research [50,62]. In the present study, the sensitivity of the parameters was assessed by varying the values of four variables: recharge, evapotranspiration, river conductance and hydraulic conductivity.

### 3.2.8. Predictive transient modelling

Using the steady-state calibrated groundwater flow model and applying the steady-state heads calculated by the model as initial heads for the transient model runs, we considered current abstraction and recharge from DIAS as an input to a transient model to test the current conditions to the best of our ability. Following this, we considered different scenarios of abstraction accounting for population/demand growth and of groundwater recharge accounting for possible changes to land use and climatic conditions (Figure 6). The intention was to test how the DIAS hydrogeological system will respond to plausible future scenarios of abstraction and recharge. The predictive transient model was performed for 30 years, representing the period 2024-2054, with changing conditions every 10 years to account for socio-environmental dynamics.

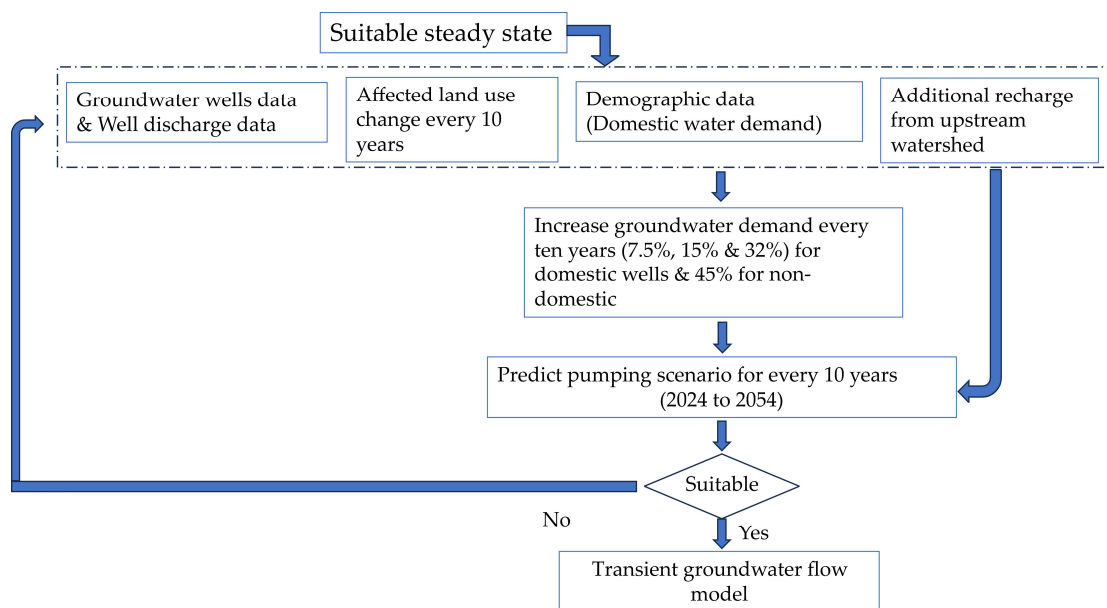


**Figure 6.** Flowchart of creation of different scenarios of groundwater abstraction and recharge

### 3.2.9. Estimation of current groundwater abstraction

Groundwater abstraction in the study is through dug wells, tubewells, and boreholes. There are three main types of abstractions, namely domestic, public supply and private for commercial enterprises (bottling water companies, hotels, etc.). Water use per capita varies significantly around the world, typically ranging from 110 to 160 liters per capita per day for middle-income households [63]. In determining the pumping rate in the MODFLOW Flex modelling in this case, the approach used refers to the daily water consumption habits of urban communities in Dili City, which we consider to be between 100 and 120 liters per person per day.

The average Dili City household consists of five to six family members [30]. Accordingly, each household's estimated daily water demand falls between 700 and 1,300 liters, or 0.7 and 1.3 m<sup>3</sup>/day. From this range, a mean value of 1.0 m<sup>3</sup>/day was chosen to serve as the modeling's representative pumping rate for domestic abstraction. This figure gives a realistic approach to the groundwater

pumping load in the flow simulation and represents typical water consumption conditions in Dili City's residential areas.

Production wells operate continuously for 24 hours a day. There is no complete pumping dataset for public supply nor commercial wells. Therefore, we estimated pumping for these types of wells based on the limited available recorded abstraction data and on maximum rates recorded in pumping tests. The amount of groundwater used by industry and pumped from different public wells varies greatly. Small industries use an average of 144 m<sup>3</sup>/day, while large industries and production wells for public water supply use an average of 576 m<sup>3</sup>/day. Thus, we used this range for input as groundwater abstraction for commercial enterprises and public supply wells on MODFLOW through the well package.

### 3.2.10. Suggested future scenarios of abstraction and recharge

We expect significant population growth in Dili, along with economic development and associated lifestyle changes. This will most likely increase groundwater demand and pumping, although it is not realistically possible to predict by how much. Thus, we created extreme but plausible scenarios, in which it was assumed that domestic pumping would increase by 32% and commercial/public supply pumping by 45% every ten years. This projection assumes an increase in domestic, commercial, and public supply pumps but also a higher rate of coverage from the public supply system, which is still limited around Dili. We increased the pumping rate in each MODFLOW well instead of adding more wells, as we don't know where new wells would be.

Climate and land use change are likely to alter groundwater recharge dynamics and rates at DIAS, although it is not possible to predict, at least with current knowledge, how that will occur. Land use changes will likely decrease infiltration due to deforestation and impermeabilization, which might lead to an increase in runoff, diminishing diffused recharge but potentially increasing localized recharge (e.g., through riverbeds). The effects of climate change in Dili are unclear, as is its impact on recharge. Thus, we considered it useful to consider three possible recharge scenarios in relation to current conditions for each 10 years of future simulations: decrease by -7.5%, increase by +7.5% and no change. Although +7.5% is an arbitrary figure, it signifies a substantial change in recharge that can generate plausible future scenarios, which help hydrogeologists, decision makers, and managers understand the aquifer's future hydrogeological conditions.

In total, nine scenarios were created with combinations of pumping and recharge rates, summarized in Table 4. Scenarios 1, 2 and 3 were run from 2024 to 2034, considering current pumping conditions and different recharge percentages compared to estimations of the current conditions (0, +7.5, and -7.5%, respectively). Scenarios 4, 5, and 6 replicate scenarios 1, 2, and 3, respectively, while introducing a modeling period from 2034 to 2044 that accounts for a 32% increase in domestic pumping and a 45% increase in commercial/public pumping, along with the same changes to recharge conditions as previously noted (0%, +7.5%, and -7.5%). Scenarios 7, 8, and 9 repeat scenarios 4, 5, and 6 (respectively) and add a modeling period from 2044 to 2054, considering a further 32% increase in domestic and a 45% increase in commercial and public pumping in relation to 2034–2044 and the same changes to recharge conditions as previously (0, +7.5%, and -7.5%, respectively).

**Table 4.** The nine different modelling scenarios suggested for the Quaternary aquifer in Dili City

A	B	C	D	E	F	G	H	I	J	K	L	M
S1	2024- 2034	1.0	144 - 576	0								
S2	2024- 2034	1.0	144 - 576	+7.5%								
S3	2024- 2034	1.0	144 - 576	-7.5%								

A	B	C	D	E	F	G	H	I	J	K	L	M
S4	2024- 2034	1.0	144 - 576	0	2034- 2044	1.32	208 - 835.2	0				
S5	2024- 2034	1.0	144 - 576	+7.5%	2034- 2044	1.32	208 - 835.2	+7.5%				
S6	2024- 2034	1.0	144 - 576	-7.5%	2034- 2044	1.32	208 - 835.2	-7.5%				
S7	2024- 2034	1.0	144 - 576	0	2034- 2044	1.32	208 - 835.2		2044-2054	32%	45%	0
S8	2024- 2034	1.0	144 - 576	+7.5%	2034- 2044	1.32	208 - 835.2		2044-2054	32%	45%	+7.5%
S9	2024- 2034	1.0	144 - 576	-7.5%	2034- 2044	1.32	208 - 835.2		2044-2054	32%	45%	-7.5%

\* Tables may have a footer. A= scenarios; B, F, J= time period; C, G, K= domestic abstractions (m<sup>3</sup>/d); D, H, L= Public/commercial Pumping (m<sup>3</sup>/d); E, I, M =delta recharge ( $\Delta R$ ).

## 4. Results

### 4.1. Conceptual model of DIAS

The simplified lithological model has shown a great correlation with the borehole lithological logs (Figure 7-a). The thickness of Quaternary sediments typically increases from south to north. Drilling data confirmed that the sedimentary basin is thicker (> 140 m) around the central to western area, while the eastern area is < 100 m. The sediments of the western area are dominated by poorly to well-sorted gravelly sand that vary in both size and composition, while the central to eastern area of Dili is formed by poorly sorted gravelly sand. The clay layer (thickness <10 m) is underlain in some areas by a thick granular zone, but the clay distribution is not continuous.

Table 5 summarizes the characteristics of the six identified lithological layers. The first layer is composed of gravelly sand with various proportions of these materials and has a thickness ranging from 1 to 68 m. The second layer is composed of clay, with a thick range from 0 to 30 m. The lateral distribution of the clay layer is uneven; it is absent in places, and it is thicker around zone two (Caicoli). The third layer consists of sand with gravel and boulders with occasional clay; the estimated thickness of this layer is 2 m to 108 m, being thicker around the Comoro area (zone one). The fourth layer is composed of unevenly distributed muddy sand mixed with clay, with a thickness ranging from 0 m to 20 m and being thicker around Zone 2 (Caicoli, Bairopite, and Hudilaran). Layer five is composed of sand with a variable thickness ranging from 24 m to 64 m, which is thicker around the Comoro area. Beneath these sediments, there is the metamorphic bedrock (layer six).

Although confined conditions may exist in specific locations, particularly in zone 2, due to the lack of monitoring data, it is not possible to distinguish between wells under confined or unconfined conditions. Thus, at the basin scale, the aquifer system can be considered to range from unconfined to semi-confined. Therefore, we modeled DIAS as an unconfined system. While this is a limitation that may be an overgeneralization, it is the best approach available with the current data. Future modeling efforts could address this issue if new data becomes available.

The observed vertical and lateral lithological variability indicates a heterogeneous sedimentary system that influences aquifer hydraulic properties. The presence of discontinuous clay layers may locally affect groundwater flow and storage conditions.

**Table 5.** Summary of DIAS' lithology units. Elevation is in meters above sea level (ASL)

Layer	Lithology/Hydrogeology	Elevation (m asl)		Thickness (m)	
		Bottom elevation.	Top elevation	Min.	Max.
1	The gravel is continuous across the entire DIAS, with different thicknesses (Figure 7-a). The elevation of the top of layer 1 was set equal to the elevation of the land surface and it represents unconfined aquifer.	-32	49.	1	68
2	The clay is not continuous across the entire DIAS, with a number of areas identified in which the clay is absent (Figure 7-a). Clay represents aquitard-1 when presents.	-38	48	0	30
3	The gravel is continuous across the entire DIAS, with different thicknesses (Figure 7-a). This layer represents unconfined to semi-confined aquifer-1.	-123	48	2	108
4	Mix of the muddy sand with clay which is not continuous across the entire DIAS (Figure 7-a). This layer represents aquitard when presents.	-85	2	0	20
5	The gravelly sand layer 2 is continuous across the entire DIAS, with different thicknesses. Layer 4 represents unconfined to semi-confined aquifer-2.	-140	23	24	64
6	Bedrock characterizes with metamorphic (shist rock), by fresh to weathered in places Represents aquifuge.	9	140	Unknown.	

Based on the subsurface lithological model (Figure 7-a), groundwater modeling is performed considering two HSU. HSU-One represents bedrock, consisting of fresh to weathered schist. It can locally store and transmit water through fractures and weathering, but it is primarily composed of fresh schist that acts as an aquifuge or is impermeable—and it is modeled as such. HSU-Two represents Quaternary deposits mainly composed of three different confined and semi-confined aquifers separated by clay layers. HSU-Two contains five layers that control groundwater flow, as described in Table 5.

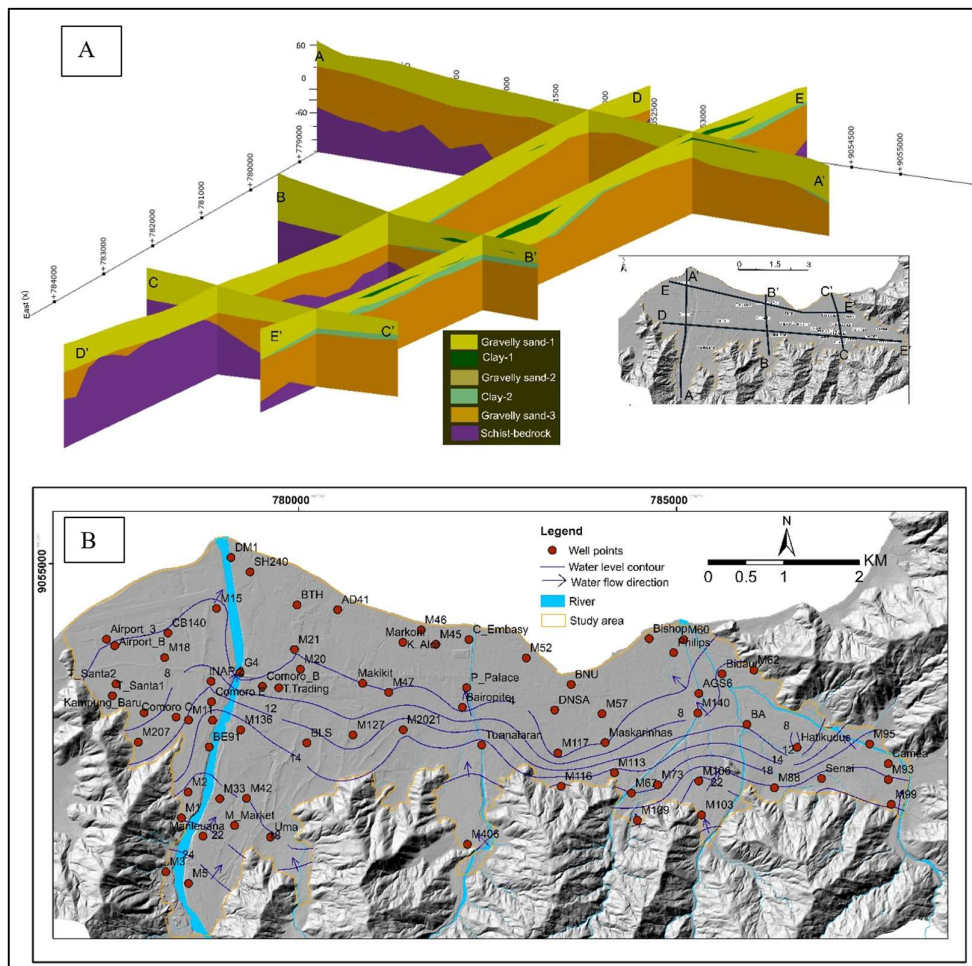


**Figure 7.** Conceptual model of DIAS: (a) Fence diagram of lithological conceptual model and (b) groundwater head contour, main rivers, flow directions and wells used for groundwater elevations.

#### 4.1.1. Groundwater level and flow direction

There is no comprehensive groundwater monitoring program in Dili. There are only four monitoring wells, of which only two are currently monitored monthly. For inaccessible wells, we assumed the groundwater level recorded after drilling was the initial water level and used it to construct the flow direction map. Otherwise, we took water level measurements, at different times of the year according to logistics. Although it is expected that static water levels may vary with the seasons, static water level measurements were considered representative of groundwater levels in the aquifer and acted as a surrogate for ambient groundwater conditions. Figure 7-b shows groundwater elevations ranging from 1 to 28 meter above sea level (masl). The general flow direction is from south to north, while it is southeast to northwest in the eastern region. Moreover, the wells located close to the coastline have a depth to the water table of ~0.5-2 m, which may allow for evaporation to occur directly from the groundwater.

#### 4.1.2. Recharge

Rainfall amounts varied from 922 to 1,229 mm/year. Real Evapotranspiration values ranged from 568 to 622 mm/year. Recharge rates are 115 mm/year in the eastern region (zone 3), 78 mm/year in the central region (zone 2), and 65 mm/year in the western region (zone 1). For the upstream of Comoro, the recharge calculated was 247 mm/year. As explained in the methodology, for considering the mountain block recharge and river infiltration in addition to the direct rainfall diffused recharge, the recharge from the upstream of Comoro was added to zone one at the same rate (resulting in a

total recharge volume reduction of 88%, due to Zone 1's smaller area compared to the total water volume available from the upstream area for recharge). These changes resulted in a total recharge rate of 312 mm/year in the western region (Zone 1). This is due to the region's size and its role as the main catchment area that carries water from the Comoro River system.

**Table 6.** Summary of recharge in the DIAS.

Zone	Stations	Average Precipitation (mm/y)	Tm (C°)	Area (km <sup>2</sup> )	Ro (mm/y)	Etr (mm/y)	Recharge	Total recharge/zone
West zone (1)	Airport	922	24.7	13	306	595	21	312
	Bemos	1133	24.0	13	429	596	109	
	Upstream of Comoro	1274	23.6	207	436	591	247	
Central zone (2)	Kakoli	1107	24.1	6	429	601	78	78
East zone (3)	Bidau	1229	24.2	7	493	622	114	115
	Becora	1158	23.4	7	474	568	117	

#### 4.2. Steady state flow model

##### 4.2.1. Calibration

Figure 8 shows a comparison of observed water levels and simulated hydraulic heads in the DIAS using a 1:1 correlation line. Table 7 shows that root mean square (RMS) and residual mean for almost all the sites during the calibration validation are low and within acceptable limits. Potential discrepancies between simulated and observed levels can be explained because of water withdrawal effects (evident in a few areas of intensive pumping), poor data availability, and errors in measurements (head) and estimations (baseflow, recharge). Initially, it was assumed that all cells in the original active zones of the model were uniformly wet. However, some of the model's original active cells, such as those in the eastern region, experienced drying out during the simulation and calibration processes. Dry cells represent areas where the water table is below the cell's bottom elevation (see Figures 9 and 10). This may occur because of the boundary conditions chosen, because there is no flow, and/or because of the hydrodynamics in this thin and elevated part of the basin.

When using the MODFLOW default value for river conductance, a very high RMS was obtained. However, when the river conductance value was manually adjusted, the analysis revealed that a higher value produced a lower RMS. In addition to the RMS results, the river conductance value affects the type of river included in the model. The rivers in the area are of the losing stream type. However, the model results that use the default conductance value do not accurately represent the losing stream type. After adjusting the river conductance value to match the losing stream type observed in real conditions, the model results better represented these hydraulic dynamics, indicating that the final conductance values were more realistic.

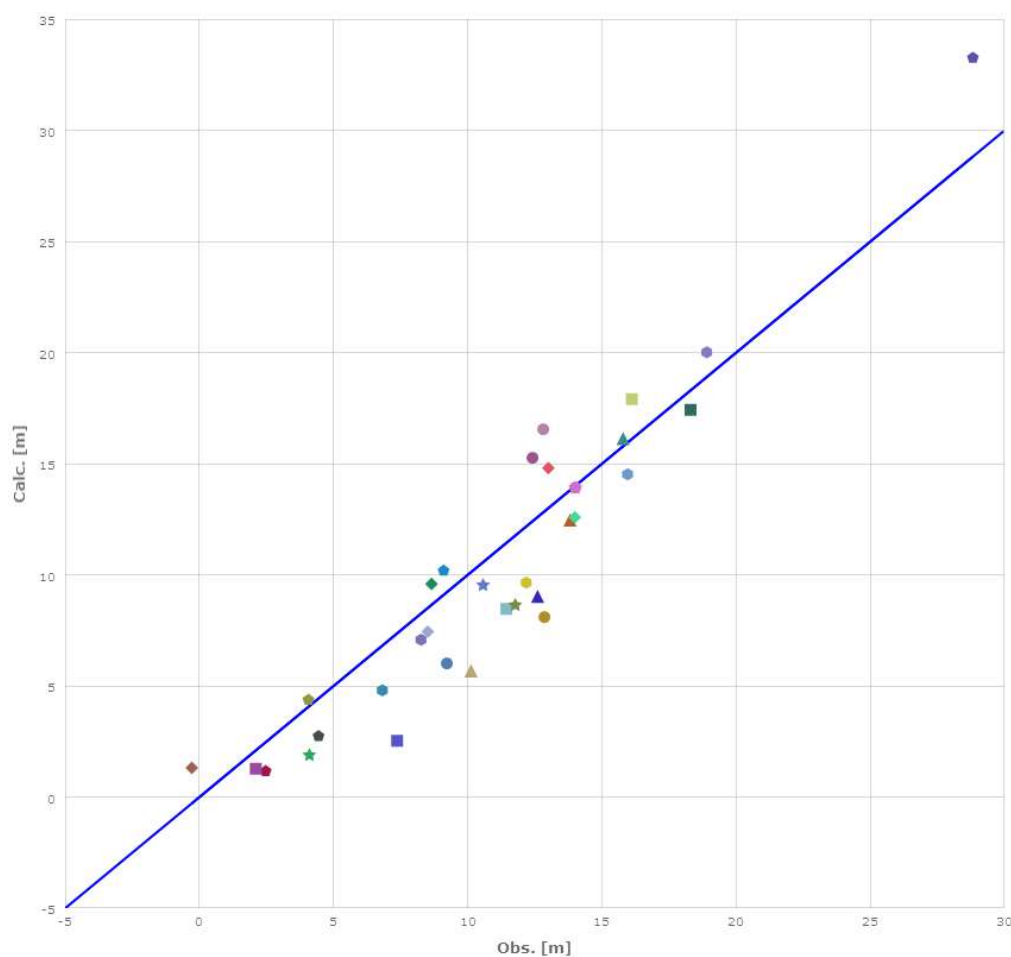


**Figure 8.** Comparison of simulated and observed hydraulic heads (calibration of 33 wells).

We tried calibrating the model using two recharge scenarios. Firstly, we considered only direct diffuse rainfall recharge to the aquifer. This procedure resulted in an error message stating that the recharge was too low and the model was unable to run. Therefore, we considered the additional recharge coming from the upper catchment of the Comoro River (Table 6), and the calibration results were satisfactory with RMS <10% (Table 7). The result is an indication that recharge originating from the upper catchment is significant for DIAS water balance. This is an example of how the numerical model can be useful for a better understanding of the conceptual model.

**Table 7.** Summary of model calibration

Standard error of the estimate	0.46	(m)
Root mean squared	2.61	(m)
Residual mean	0.34	(m)
Number of data points	33	
Normalized root mean squared	8.98	(%)
Min residual	-0.04	(m)
Max residual	5.22	(m)
Correlation coefficient	0.91	
Abs. residual mean	2.14	(m)

#### 4.2.2. Modeled groundwater balance

Recharge to the aquifer system is from precipitation, at 103 mcm, and river leakage, at 169 mcm. The total inflow to the aquifer is 272 mcm and the total outflow is 273 mcm (see Table 8). This results in a quasi-neutral water balance of  $\Delta S = -1$  mcm, which is consistent with what is expected in steady state – this  $\Delta S$  represents 0.4% of the total inputs/outputs, which can be considered negligible seeing the data limitations and assumptions in the model. Table 8 shows significant outflow to the sea and no inflow, as well as significant infiltration from the rivers and outflow from the aquifer to the rivers depending on  $K$  and available water resources. There is also significant loss of water through evapotranspiration directly from the water table, which is not surprising given the very shallow water tables near the coast. The model shows that rivers mainly supply groundwater, which is consistent with the above remarks regarding losing conditions and field observations of river dynamics.

**Table 8.** Steady-state groundwater budget for 14 years (2009-2023).

No	Water balance component	In (mcm)	Out (mcm)	$\Delta S$ (mcm)
1	Constant Head (sea boundary)	0	144	-144
2	River Leakage (infiltration)	169	68	101
3	Evapotranspiration (from water table)	0	61	-61
4	Recharge	103	0	103
5	Total	272	273	-1

#### 4.2.3. Groundwater level variation

The numerical model is an unique tool for understanding the spatial distribution of groundwater heads over time and according to different aquifer stresses (e.g., pumping, recharge) and boundaries. According to the steady-state model (Figure 9), the groundwater regime has the same general flow directions, from southwest to north, and is consistent with measured levels (Figure 7-b), with groundwater levels ranging from 0 to 66 m (Figure 9).

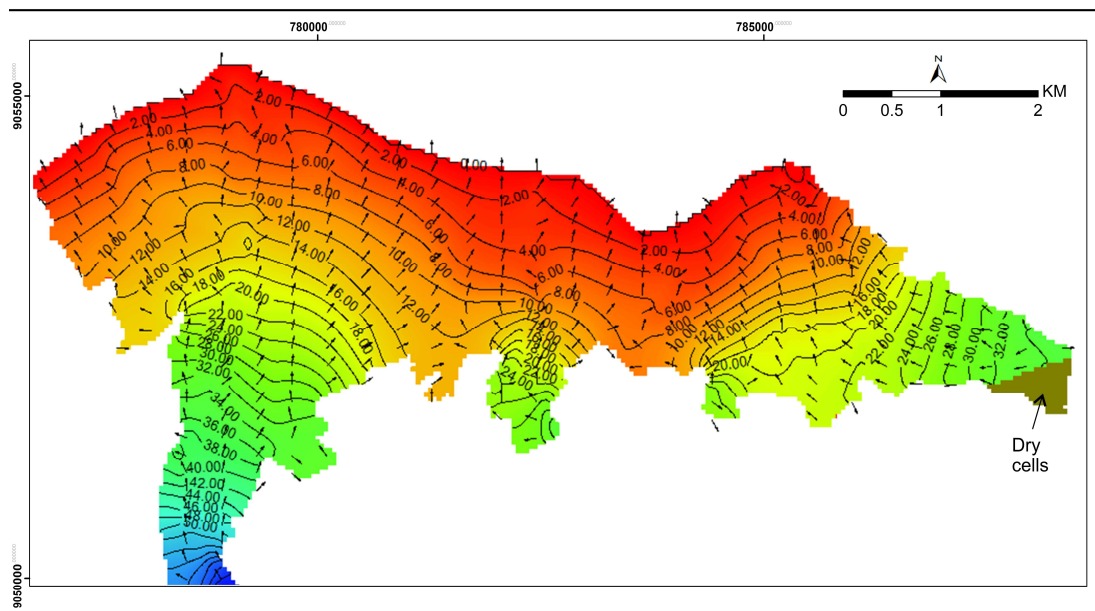


**Figure 9.** Simulated steady-state groundwater levels in DIAS.

### 4.3. Transient model and scenario testing

The results in Table 9 and Figure 10a demonstrate the significant impact of pumping on the water balance of the system. Introducing pumping at the estimated current rates and maintaining recharge unaltered resulted in  $\Delta S = -27$  mcm by 2034. Increasing pumping created stronger groundwater deficits of  $-30$  mcm by 2044 and  $-34$  mcm by 2054 (Figure 11), indicating greater stress on the DIAS, especially in zones two and three where the water supply is deteriorating (see Figure 10). Infiltration from rivers is the main source of water in the system. Interestingly, outflow to the sea is the main water loss by 2034 and 2044, while abstraction becomes the main outflow by 2054, which is an indication of potential seawater intrusion as abstraction increases. As shown in Figure 10, several areas along the northern coast, including Madohi, K. Alor, Fatuhada, Farol, and Formosa, are at risk of saltwater intrusion due to the declining water table.

**Table 9.** Summary of water balance for scenarios 1, 4, 7 – increasing pumping and current recharge

S1 - Year 2024-2034 (Recharge + 0)			
Parameter	IN (mcm)	Out (mcm)	$\Delta S$ (mcm)
Constant head (Sea boundary)	0	71	
Abstractions	0	49	
River leakage	99	29	
ET (from aquifer)	0	28	
Recharge	52	0	
Total	151	178	-27
S4 - Year 2024-2044 (Recharge + 0)			
Parameter	IN (mcm)	Out (mcm)	$\Delta S$ (mcm)
Constant head (Sea boundary)	1	132	
Abstractions	0	118	
River leakage	217	52	
ET (from aquifer)	0	50	
Recharge	103	0	
Total	321	351	-30
S7 - Year 2024-2054 (Recharge + 0)			
Parameter	IN (mcm)	Out (mcm)	$\Delta S$ (mcm)
Constant head (Sea boundary)	1	188	
Abstractions	0	212	
River leakage	350	71	
ET (from aquifer)	0	70	
Recharge	155	0	
Total	506	540	-34

Despite the increase in pumping, the results from Table 10 and Figure 10 b show that the increase in recharge has a strong effect over time, contributing to a less negative  $\Delta S$ :  $-25$  mcm by 2034,  $-24$  mcm by 2044 and  $-21$  mcm by 2054 (Figure 11). The results indicate that recharge is a key aspect influencing the water balance and maintaining the sustainability of the system. Thus, significant future efforts should be invested to obtain more accurate estimations, and consequently reduce uncertainty around aquifer dynamics, and in measures to increase recharge. Infiltration from the rivers is the main source of water to the system. In line with S1, S4 and S7, these simulations show that outflow to the sea is

the main water loss by 2034 and 2044, while abstraction becomes the main outflow by 2054, which is an indication of potential seawater intrusion as abstraction increases even if recharge also increases.

**Table 10.** Summary of water balance for scenarios 3, 6, 9 – increasing pumping and increased recharge.

<b>S3 - Year 2024-2034 (Recharge + 7.5%)</b>			
<b>Parameter</b>	<b>IN (mcm)</b>	<b>Out (mcm)</b>	<b><math>\Delta S</math> (mcm)</b>
Constant head (Sea boundary)	1	77	
Abstractions	0	49	
River leakage	106	32	
ET (from aquifer)	0	31	
Recharge	56	0	
Total	162	187	-25
<b>S6 - Year 2024-2044 (Recharge + 7.5%)</b>			
<b>Parameter</b>	<b>IN (mcm)</b>	<b>Out (mcm)</b>	<b><math>\Delta S</math> (mcm)</b>
Constant head (Sea boundary)	1	142	
Abstractions	0	118	
River leakage	233	56	
ET (from aquifer)	0	54	
Recharge	111	0	
Total	345	369	-24
<b>S9 - Year 2024-2054 (Recharge+ 7.5%)</b>			
<b>Parameter</b>	<b>IN (mcm)</b>	<b>Out (mcm)</b>	<b><math>\Delta S</math> (mcm)</b>
Constant head (Sea boundary)	2	202	
Abstractions	0	212	
River leakage	376	76	
ET (from aquifer)	0	75	
Recharge	167	0	
Total	544	565	-21

The results from Table 11 and Figure 10 c show that the decrease in recharge has a strong effect over time, contributing to an increasingly negative  $\Delta S$ : -28 mcm by 2034, -37 mcm by 2044 and -47 mcm by 2054 (Figure 11). The results show that if recharge decreases overtime, the sustainability of the system is threatened. This is a further indication that significant future efforts should be invested to obtain more accurate estimations, and consequently reduce uncertainty around aquifer dynamics, and in measures to increase recharge. Infiltration from the rivers is the main source of water to the system. In line with S1, S3, S4, S7 and S9, these simulations show that outflow to the sea is the main water loss by 2034 and 2044, while abstraction becomes the main outflow by 2054, which is an indication of potential seawater intrusion as abstraction increases and recharge decreases. S8 represents the worst-case scenario for the water balance according to the assumptions considered, combining the highest abstraction with lowest recharge rates.

**Table 11.** Summary of water balance for scenarios 2, 5, 8 – increasing pumping and decreased recharge Year 2024-2034 (Recharge -7.5%).

<b>S2 - Year 2024-2034 (Recharge-7.5%)</b>			
<b>Parameter</b>	<b>IN (mcm)</b>	<b>Out (mcm)</b>	<b><math>\Delta S</math> (mcm)</b>
Constant head (Sea boundary)	0	66	
Abstractions	0	49	
River leakage	91	27	
ET (from aquifer)	0	26	
Recharge	48	0	
<b>Total</b>	<b>140</b>	<b>168</b>	<b>-28</b>
<b>S5 - Year 2024-2044 (Recharge- 7.5%)</b>			
<b>Parameter</b>	<b>IN (mcm)</b>	<b>Out (mcm)</b>	<b><math>\Delta S</math> (mcm)</b>
Constant head (Sea boundary)	1	122	0
Abstractions	0	118	0
River leakage	200	48	0
ET (from aquifer)	0	46	0
Recharge	96	0	0
<b>Total</b>	<b>297</b>	<b>334</b>	<b>-37</b>
<b>S8 - Year 2024-2054 (Recharge- 7.5%)</b>			
<b>Parameter</b>	<b>IN (mcm)</b>	<b>Out (mcm)</b>	<b><math>\Delta S</math> (mcm)</b>
Constant head (Sea boundary)	1	174	
Abstractions	0	212	
River leakage	323	66	
ET (from aquifer)	0	64	
Recharge	143	0	
<b>Total</b>	<b>468</b>	<b>515</b>	<b>-47</b>

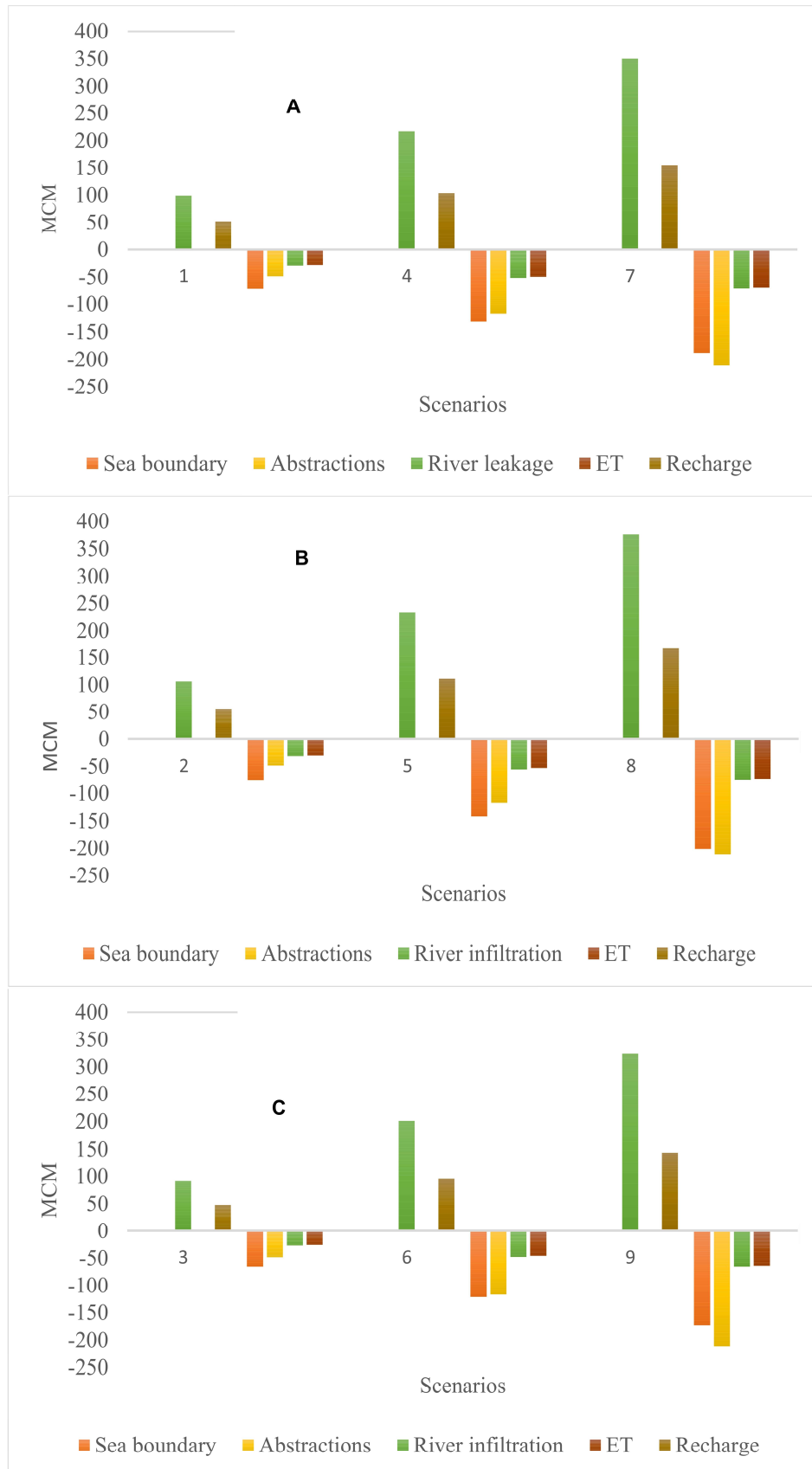


**Figure 10.** Water balance simulations for the nine predictive scenarios. A) scenarios 1, 4, 7; B) scenarios 2, 5, 8 and C) scenarios 3, 6, 9.

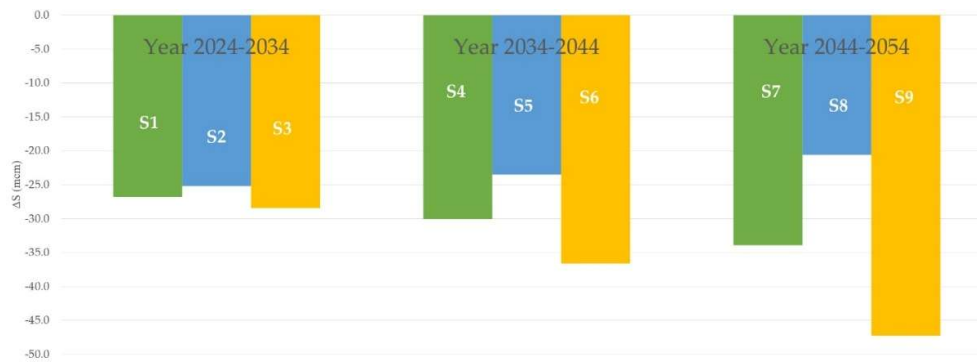


Figure 11.  $\Delta S$  results for Scenarios 1–9.

Figure 10 shows the water balance for all scenarios, according to the different components. It illustrates that river leakage is a strong component of the water balance, as the main source of water input into the system. This is compatible with field observations that large volumes of water flow through the rivers during the wet season and infiltrate quickly. Thus, it is crucial that future studies focus on estimating the potential for river infiltration more accurately and on surface-groundwater interactions more generally. Reducing river infiltration uncertainty will reduce water balance and conceptual uncertainty greatly and will allow for (better) aquifer management. As for outflows, flow to the sea and abstractions are the main components, depending on which scenario we consider. Thus, it is critical to have better estimates of groundwater pumping in Dili to constrain the water balance properly. A future numerical groundwater model considering density differences between fresh groundwater and seawater will also be important to better estimate discharge to the sea, and the risk of seawater intrusion – although that is of limited relevance until meaningful monitoring datasets exist.

Figure 9 shows the distribution of groundwater levels for the steady-state model, while Figure 12 shows equivalent maps for the nine different scenarios. Table 12 summarizes the variation in groundwater levels for the different scenarios according to the aquifer zones. The comparisons below are in relation to transient groundwater levels.

In scenario 1 (current pumping and recharge) the groundwater flow pattern remains similar to steady state (Figure 12a). Groundwater head ranges from 0 to 66 masl around zone 1, from 0 to 27 masl around zone 2, and from 0 to 33 masl around zone 3.

Scenario 2 (current pumping, +7.5% recharge) shows increased groundwater heads (Figure 12b) of 1-2 masl around zone 1, of 2-3 masl around zone 2, and of 2-3 m around zone 3.

Scenario 3 (current pumping, -7.5% recharge) shows a decline in groundwater levels (Figure 12c). Groundwater head drops by approximately 1–3 masl (the red zone narrows) around zone 1. There is a more noticeable drop in head, along with dense contours and steep gradients, around zone 2, where the head drops by approximately 2–3 masl. The green-yellow zone shifts northward around zone 3 (Table 12). The noticeable differences include the 12 m contour line around zone 1, which shifted ~100 m to the south due to water extraction from boreholes INAP 1 and 2, Acad Policia, G4, Top Fresh, and Comoro A; the 34 m contour line around the Comoro River also moved south by ~40 m; the 8-meter contour line moved southward around zone 2; in zone 3, the 22 m contour line shifted eastward, closely followed by the 20 m contour line near borehole Becora and Kuluhun; and in the same zone, contour lines between 30 and 32 m exhibited a similar pattern.

In scenario 4 (Figure 12d) (increased pumping, current recharge), groundwater heads show little differences.

Scenario 5 (Figure 12e) (increased pumping, +7.5% recharge) shows groundwater heads increase 1-2 masl around zone 1, the head increases 2-3 masl with sparse contour around zone 2 and the head increases 3-4 masl around zone 3.

Scenario 6 (Figure 12f) (increased pumping, -7.5% recharge) shows accelerated decline in groundwater levels by 1-3 masl around zone 1, by 2-4 masl around zone 2 and by 2-3 masl around

zone 3 (Table 12). A cone of depression is observed around zone 1 due to abstractions, and the 12 m contour line shifted southward ~ 200 m. In zone 2, the 10 m contour line shifted southward ~ 50 m and the 16 m contour line around zone 3 is also shifted southward ~ 50 m.

For scenario 7 (Figure 12g) (further increased pumping, current recharge), the system remains stable but groundwater levels are trending downward, where cones of depression appear around zones 1 and 3.

Scenario 8 (Figure 12h) (further increased pumping, +7.5% recharge) shows head increases by 1–2 masl around zone 1 and by 2–3 masl around zones 2 and 3. In this scenario is noticeable that the 4 m contour line shifted northward around Zone 2, as did the 16 m contour line around Zone 3.

Scenario 9 (Figure 12i) (further increased pumping, -7.5% recharge) shows a drop in the groundwater head of 1–3 masl around zone 1, 2–4 masl around zone 2 and 2–3 masl around zone 3. This resulted in the 4 m contour line being shifted southward in zone 2, while the 16 m contour line was also shifted southward, forming a cone of depression around zone 3. There is also the formation of a cone of depression between contour lines 8 and 12 m in zone 1, which includes the INAP 1 and 2 wells, the Acad Policia well, the G4 well, the Top Fresh well, and the Comoro A and B wells.

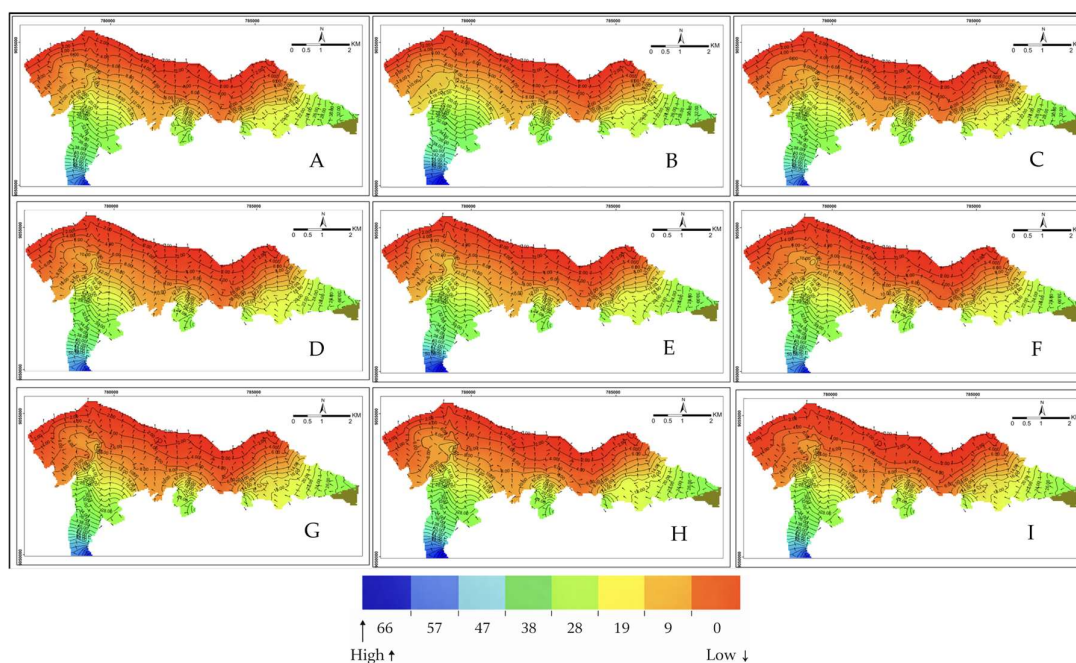


Figure 12. Simulated groundwater levels for Scenarios 1–9

Table 12. Quantitative comparison of simulated groundwater levels for the 9 scenarios for each zone.

2024-2034			
Zones	-7.5% Recharge	Current Recharge	+7.5% Recharge
Zone 1	Head drops ~1–3 m, red zone narrows	Head 0 to 66 masl	Head rise ~1 to 2 m and expands
Zone 2	The most noticeable drop in head, dense contours, steep gradients	Head 0 to 27 masl	Head rise ~2 to 3 m, less frequent contour lines
Zone 3	Head down ~2–3 m, green–yellow zone shifts northward	Head 0 to 33 masl	Head rises ~2 to 3 m, green–yellow zone expands
2024-2044			
Zones	-7.5% Recharge	Current Recharge	+7.5% Recharge
Zone 1	Head ↓ 1 to 3 m	Head 0 to 18 masl	Head ↑ 1 to 2 m

Zone 2	Head ↓ 2 to 4 m, dense contours	Head 0 to 24 masl	Head ↑ 2 to 3 m, sparse contour
Zone 3	Head ↓ 2 to 3 m	Head 0 to 30 masl	Head ↑ 3 to 4 m
<b>Hydraulic gradient</b>	Steep	Medium	Gentle slope
<b>2024-2054</b>			
<b>Zones</b>	<b>-7.5% Recharge</b>	<b>Current Recharge</b>	<b>+7.5% Recharge</b>
Zone 1	Head ↓ 1 to 3 m, Cone of depression	0 to 16 masl	Head ↑ 1 to 2 m
Zone 2	Head ↓ 2 to 4 m	0 to 20 masl	Head ↑ 2 to 3 m
Zone 3	Head ↓ 2 to 3 m, Cone of depression	+0 to 26 masl	Head ↑ 2 to 3 m
<b>Hydraulic gradient</b>	Steep	Medium	Gentle slope

Comparisons between current and changed recharge conditions over a 10-year period (2024–2034) show that reducing recharge by 7.5% results in a significant decrease in groundwater levels, particularly in zones 1 and 2. Conversely, a 7.5% increase in recharge shows the opposite effect. The results consistently identify the western Comoro area (zone 1) as the primary recharge zone, while zones 2 and 3 showed less recharge. The results of the 20-year models (scenarios 4, 5 and 6) show the same trends: a decrease in recharge of 7.5% leads to a significant drop in groundwater levels in zones 1 and 2, while an increase in recharge of 7.5% stabilizes the system. Zone 1 continues to act as the dominant recharge zone, while zone 3 is the most sensitive to recharge fluctuations.

Reduced recharge accelerates depletion, most prominently in zone 2, over a 30-year period (2024–2054), making conservation strategies even more critical. Conversely, increased recharge increases aquifer reserves and maintains the hydraulic gradient. Across all tested timeframes, zone 1 consistently functions as the main recharge area, while zone 2 becomes the primary discharge zone and experiences the most pronounced fluctuations. Zone 3 also benefits significantly from increased recharge, as evidenced by its clear up-and-down responses.

## 5. Discussion

### 5.1. Comparison with previous modelling of DIAS

Despite a previous attempt to model DIAS, our work is highly relevant and novel because our modelling objectives, methodologies, datasets, complexity, boundary conditions, lithological heterogeneity, various recharge mechanisms, future scenarios, and results differ significantly [24], as summarized in Table 13. A key distinction between the studies is the objectives, which in our case were to refine the conceptual model using the numerical model and understand the hydrological variables that are more influential for the water balance, while theirs were to estimate safe/sustainable yield. All model choices and datasets have a strong influence on the results. An important example of a fundamental difference is the sea boundary, which we modeled as a fixed head, and modeled it as free drainage [24]. It is reasonable to assume that the average sea level fixes the head at sea, a common practice in modeling. An important consequence of this distinction is the water inflowing from the sea to the aquifer in our model, which in a simple way (because we did not consider density differences) represents potential seawater intrusion, an important threat for the sustainability of this coastal aquifer. This scenario was not identified because of the different boundary condition choices [24].

We recognize we benefited from having more robust and complete datasets, and thus we were able to create a more complex and realistic numerical model. The model takes into account

lithological heterogeneity, various recharge mechanisms, boundary conditions, and future scenarios involving different recharge rates and pumping activities. Nonetheless, we acknowledge the importance of the first modelling attempt, according to the data available to them [24], which allowed us to improve upon their work (Table 13).

**Table 13.** A comparison of the current study with the previous modelling study.

	Previous study [22]	Current work
<b>Objectives</b>	(i) to develop a well calibrated groundwater flow model of the area;	(i) to understand the conceptual model better, and which variables might impact the water balance more (e.g. recharge, evapotranspiration, hydraulic properties, abstraction rates and locations, hydrostratigraphy);
	(ii) to estimate safe yield and sustainable yield.	(ii) to predict changes to the water balance according to different scenarios of recharge, land use and abstraction changes;
		(iii) to propose future work, arising from the knowledge and uncertainties here gained, that allow for further inquiry into the hydrogeology of the system and more-informed management decisions.
Boundary conditions	(i) River boundary (Kuluhun, Comoro and Bidau)-specified head boundary.	(i) River's boundary (Maloa, Lahene, Kuluhun/Taibesi, and Becora/Bidau rivers)-specified head boundary
	(ii) Sea boundary - head dependence flux boundary/free drainage,	(ii) Sea boundary - constant head;
	(iii) West, south and east boundary - specified flux	(iii) West, south and east boundary –no flow
Number of wells (for calibrations)	5 wells	33 Wells
Calibration period	2008-2013 with seasonal time steps	2009-2023
Horizontal discretization	Discretized to 63 rows and 120 columns	Discretized to 125 rows and 250 columns. The total number of cells over the area is 31,250, with each cell measuring 45 m x 45 m in each layer
Lithological layers	A top sandy gravel layer and bottom clay layer, without specifying thickness or spatial distribution. The second layer comprises mainly of saprolite (clay).	The analysis is based on drilling logs used for lithological modelling. Numerical model considers six layers, alternating gravelly sand and clay, and the bedrock.
Weather data	Seven weather stations (2003-2014)	Five weather stations (2021-2023) and 4 weather stations for the upstream Comoro catchment (2012-2019)

	Previous study [22]	Current work
Hydraulic conductivity	Default value of 0.0001 m/day	Range from $3.5 \times 10^{-7}$ to $8.5 \times 10^{-3}$ m/s, according six different layers (see Table 2)
Recharge calculations	Methodology not indicated.	Using equations to calculate recharge based on rainfall, run-off and evapotranspiration.
Recharge mechanisms	Direct diffused recharge from rainfall	Direct recharge from rainfall, river infiltration and mountain block recharge
Steady state period	2009-2013	2009-2023
Future scenario tested	Five scenarios of abstractions increase from 10 to 50 %. The modelling period is not mentioned. Recharge remained constant.	Nine scenarios, where the recharge varies from -7.5 to +7.5% and the abstraction varies from 32 up to 45%. Modelled period from 2024 to 2054.
Spatial data (topography)	Digital Elevation Model (ASTER DEM) (Spatial resolution: 30m x 30 m; Year: 2011)	LIDAR (Spatial resolution: 5m x 5 m; year 2014)
Pumping considers		
A. Public/commercial	A – Yes: (14 wells), pumping rate 0.23 m <sup>3</sup> /s	A – Yes: (46 wells), pumping rate from 144 to 576 m <sup>3</sup> /day
B. Domestic	B – Not provided	B – Yes (3557 wells), pumping rate 1.0 m <sup>3</sup> /day
Conceptual model		
A. Lithological model	A. No lithological model is presented	A. Lithological model is presented (see Figure 7.a)
B. Recharge	B. Recharge assumed to be homogenous across the basin of 118 mm/y	B. Recharge: 312 mm/year for Zone 1, 78 mm/ year for Zone 2, and 115 mm/year for Zone 3.
Safe yield	Yes	No
Scenarios period	Not provided	Year 2024-2054
<b>Results</b>		<ol style="list-style-type: none"> <li>Monitoring: groundwater &amp; salinity, climate variables, groundwater &amp; surface water interaction and abstractions.</li> </ol>
Suggestions for future work	Not provided	<ol style="list-style-type: none"> <li>Conceptual understanding: recharge rates &amp; processes, confined &amp; unconfined conditions, hydraulic properties heterogeneity &amp; risk of sea water intrusion.</li> <li>Modeling: Sea water intrusion, recharge modeling, surface water modeling, automatic calibration and contamination modeling and effectiveness of different groundwater management approaches.</li> </ol>

	Previous study [22]	Current work
Suggestions for management	<p>SGy to sustain groundwater development in the Dili aquifer is likely to be within a range of 0.23 to 0.28 m<sup>3</sup> /s.</p> <p>Conjunctive use of surface water and groundwater; and utilizing excessive runoff in wet season to increase groundwater storage by artificial recharge techniques</p>	<p>(i) Thorough monitoring networks; (ii) regulation policies for pumping and drilling; (iii) measures to increase recharge and minimize flooding (e.g. reforestation of the river catchments, development of infiltration ponds throughout the catchments, prevention of soil impermeabilization and erosion, and structures throughout the rivers to gradually promoting infiltration); and, (iv) to invest in thorough groundwater studies</p>

In what relates to recharge, our study is the first to distinguish three different recharge zones for the DIAS and to mention mountain-block recharge as a relevant mechanism (Table 6). We calculated recharge using empirical recharge estimation methods outlined in equations 1-4. The current study indicates a recharge rate of 312, 78, and 115 mm/year for zones 1, 2, and 3.

A previous study reported a recharge rate of 107 mcm/year based on the hydrological water balance method [16]. Another study reported recharge rates of 118 mm/year, despite not specifying the method [24]. Our study demonstrates that recharge and infiltration from rivers are essential elements of the water balance and should be integral considerations in future hydrogeological research and management strategies for DIAS, a point overlooked in prior studies.

### 5.2. Implications of the model for the sustainable use of groundwater

The numerical model here presented is, to the best of our knowledge, the most advanced tool for sustainable groundwater management in Dili, and anywhere in Timor-Leste. The main implications for sustainable groundwater management arising from this model are discussed as follows.

The western zone of the aquifer is more productive, and has higher groundwater potential, than the central and eastern zones due to its recharge dynamics. Consequently, if water extraction increases across DIAS, the water levels are expected to fall in the central and eastern zones over the next 30 years (Figure 9), which is depicted by the model's ability to forecast spatio-temporal changes in groundwater levels and flow directions. The model also shows that the north coast could be contaminated by seawater if extraction increases (Figure 9). As shown before, there is very little data hydrogeological data for the central and western zones, including a record of domestic wells, and as such acquiring more data for those areas is essential for aquifer protection.

The model evaluates potential impacts of climate and land-use changes, and water use, through different groundwater recharge and abstraction scenarios. When recharge drops, while extractions stay the same or increase, DIAS extraction rates exceed recharge capacity. Different water usage scenarios involving domestic and non-domestic users show the negative impacts of over-abstraction, providing useful evidence for setting groundwater extraction limits and establishing zoning policies. Three scenarios (S2, S5, and S8) specifically showed that the north and central regions can be drastically affected, with maximum drawdowns of 6 to over 10 m.

The model shows recharge, directly from rainfall, through river infiltration and/or from mountain-block processes, is a key component of the water balance. Thus, significant effort needs to be put into characterizing recharge processes and calculating recharge rates better. Furthermore, creating conditions that allow for greater recharge will significantly impact the aquifer's long-term sustainability. Such an effort could involve reducing impermeable areas in Dili, increasing infiltration throughout the river catchments (e.g., through reforestation and riverbank and soil protection),

reducing river flow velocity and increasing infiltration in riverbeds. The measures to increase recharge would have the multipurpose of helping to reduce and manage flood risk, which is a chief water-related problem in Dili, and a threat to property and human lives. As majority of DIAS's water supply relay on groundwater, a comprehensive groundwater management strategy is therefore required, considering environmental, technical, social and political factors. So far, the policymakers may have drafted policy, but it has not been translated into reality. For instance, the amount of groundwater abstraction in each zone remains undefined. Moreover, Dili is characterized by poor urban plans and a lack of wastewater management that can cause the shallow groundwater to be contaminated [21,22]. This study can assist policymakers in estimating sustainable extraction levels to prevent over-extraction, especially in the central and northern parts of the DIAS. Policymakers are also suggested to draft and enforce drilling policies to control and organize groundwater drilling activities, and to collect drilling data and create databases for increasing the hydrogeological knowledge and to keep understanding the evolving nature of the state of the aquifer system. Acquiring climatic data and crating databases shared across institutions is also fundamental to understand the aquifer system dynamics, which are presently nonexistent. It is necessary to improve groundwater levels and quality (e.g. salinity) monitoring to effectively control groundwater abstractions and their impacts on the aquifer. The groundwater monitoring system is important for (i) assessing the state of the aquifer in terms of how it will respond to pumping and recharge; (ii) evaluating the risk of seawater intrusion, contamination, and water availability for domestic purposes; (iii) evaluating the recharge and discharge dynamics from the river to the aquifer; and, (iv) monitor areas with larger aquifer withdrawals, as indicated by cones of depression. We propose the groundwater monitoring system shown in Figure 13, which is based on scenario modeling for the worst-case scenario (scenario 9 – low recharge, high abstraction). Ultimately, the management strategy should promote groundwater conservation and efficient use, and prioritize storage enhancement and distribution capacity to sustainably meet the population and environmental needs.

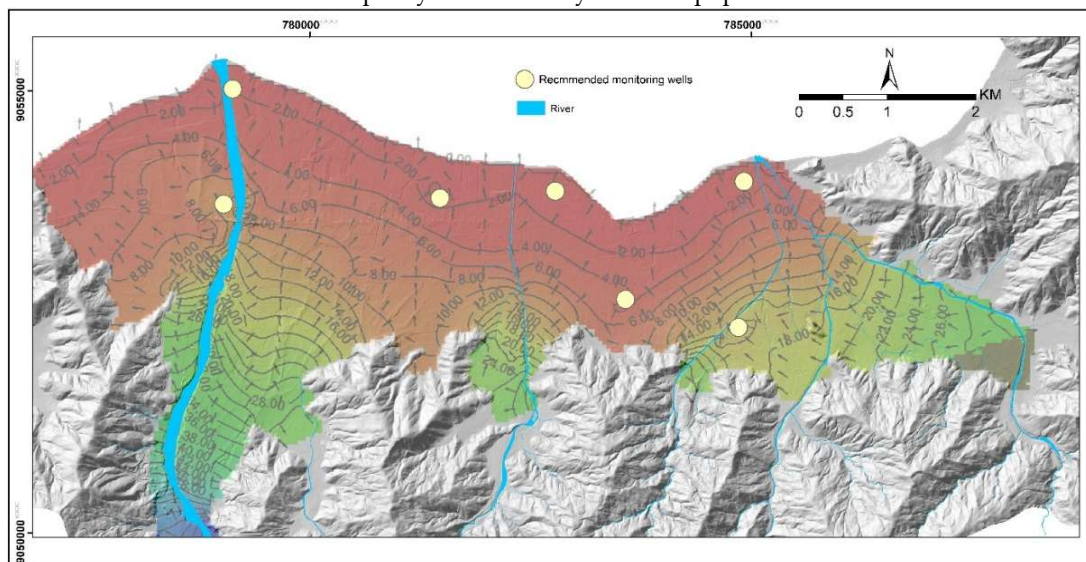


**Figure 13.** Proposed location of monitoring wells based on the dynamic of groundwater levels.

### 5.3. Limitations and the uncertainties in the model

The modelling attempt here presented is affected by severe limitations, the chief being data availability: (i) there is no groundwater monitoring network in Dili (only two wells are being measured monthly); (ii) there are very few measurements of pumping data; (iii) there is no register of domestic wells; (iv) there is no public register of drilling reports or well logs; (v) there are no river flow measurements; (vi) there is no continuous and comprehensive climatic monitoring; (vii) there is no field-based data that allows for the estimation of recharge, and spatio-temporal variability, with typical methods, such as the chloride mass balance or water-table fluctuation, and for the estimation

of mountain-block recharge; (viii) there is no data on seawater intrusion; and, (ix) there is very limited information to distinguish between unconfined and confined conditions.

These data-availability limitations impact the ability to model the system accurately. Thus, the model here present can be considered an initial model that explores the conceptual uncertainties of the hydrogeological system but also that provides a solid base for future, more complex modelling efforts. The main limitations of this model are: (i) recharge was calculated with a single method based on limited, short-term local climatic data, which allowed very little insight into spatio-temporal variability and mountain-block recharge; (ii) many assumptions have to be made about abstractions from the system, as very incomplete data exist on this; (iii) despite the thousands of wells existing in Dili, we only had access to 157 to model the lithostratigraphy of the basin, which limited our ability to do so comprehensively at the basin scale; (iv) very little data exist on the aquifer hydraulic properties and their spatial variability, and as such we used the few pumping tests available and literature values to characterize the aquifer; (v) as this is an initial modelling effort, and with little data, we did not consider density differences and seawater intrusion, although this model sets the basis for such types of modelling considerations in the future; and (vi) as there are no measurements of river flow, the model is very limited in the ability to model the interactions between surface and groundwater, especially river infiltration and aquifer discharge.

Despite this long list of important limitations, the model represents a significant increase in the hydrogeological understanding of the Dili basin, including conceptual and how it may respond to climatic and abstraction stresses in decades to come. We consider it a fundamental tool for building new knowledge upon, and for science-informed groundwater management.

Based on the study's findings, further research is needed in the areas of monitoring, conceptual understanding, modelling and management. As for monitoring, we suggest future work to include: (i) a comprehensive monitoring network of groundwater levels and salinities, potentially including data loggers in strategic wells, including assessing the potential for sea water intrusion, and water-table fluctuations for groundwater recharge estimation; (ii) comprehensive monitoring of climate variables, both in the Dili area and upstream in the Comoro catchment, which can include collection of rainfall samples for characterizing rainwater quality and calculating recharge through the chloride mass balance method; (iii) a monitoring network of surface-groundwater interactions and how it changes throughout the year according to climate variability; and, (iv) monitoring of abstraction in a selection of public, commercial and domestic wells.

The monitoring efforts mentioned above can assist in a better conceptual understanding of DIAS. The main conceptual questions are: (i) what is the spatio-temporal variability of recharge?; (ii) What are the dynamics and rates of mountain-block recharge?; (iii) What are the dynamics of surface-groundwater interactions, and how do they influence recharge and discharge?; (iv) What areas are more at risk of seawater intrusion?; (v) In which zones do we find confined conditions, and how do hydraulic properties vary spatially with lithology, including in the riverbeds?; and, (vi) How do groundwater levels change throughout the year according to climate and pumping variability?

Comprehensive monitoring and enhanced conceptual understanding will allow for more robust modeling. Aspects to be developed in future modelling efforts are (i) density-driven seawater intrusion modelling; (ii) surface water flow modelling; (iii) fully coupled surface-groundwater modelling; (iv) automatic modelling calibration; (v) recharge modelling; (vi) a groundwater model considering unconfined and confined conditions; (vii) a model testing more complex scenarios of future recharge and demand and impacts on aquifer depletion, seawater intrusion and interactions with surface water; (viii) a model testing the effectiveness of different groundwater management approaches; and, (ix) contamination modelling.

## 6. Conclusions

Hydrogeological conceptual and groundwater flow modeling are essential tools for assessing groundwater availability and quality, understanding the processes controlling groundwater behavior, and ensuring the protection of groundwater resources. This approach was here applied to

the coastal urban area of DIAS, which lacks groundwater management, has very little data and monitoring, and faces increasing unregulated groundwater drilling and abstraction. The current study, through lithological and numerical modeling, increases the conceptual understanding of DIAS' hydrological system, highlights the knowledge gaps and data needs, illustrates the main processes controlling groundwater behavior and the water balance, and predicts the groundwater response to future scenarios of increased abstraction and variable recharge. Importantly, it provides recommendations for future work, including monitoring, conceptual understanding, modeling, and management approaches. The present study is an essential tool to assist policymakers in the sustainable development of water resource management and mitigating environmental risks in the city of Dili. It can serve as guidance in how to study similar aquifer systems in the world where little data and conceptual understanding exist.

The lithological model reveals that unconsolidated sediments such as gravelly sand, clay, and muddy sand, deposited above metamorphic bedrock, form the DIAS. The aquifer system consists of three unconfined to semi-confined aquifers, intercalated by two semi-confining aquitard layers. The bedrock is considered an aquifuge with low hydraulic conductivity. DIAS can be divided into three zones according to river catchments (five rivers flow into Dili's sedimentary basin). Zone one has the thickest part of the sedimentary basin. It is characterized by poorly to well-sorted sediments, with thinner clay layers and thicker aquifers. Zones two and three are characterized by poorly-sorted sediments, with thicker clay layers and thinner aquifers. Thus, zone one has the highest aquifer potential in Dili. This portion is lithologically related to the alluvial plains of the Comoro River, the biggest in the region. The rivers flow from south to north, and so does groundwater.

Rainfall-distributed recharge rates were, based on climatic data, estimated to be variable across the aquifer: 65 mm/year for zone one, 78 mm/year for zone two, and 115 mm/year for zone three. Infiltration from the rivers and mountain-block recharge are additional recharge processes in the system, although there is virtually no data to calculate these. Recharge for the upper catchment of the Comoro River was calculated as 247 mm/year, and we added a portion of this recharge as an input to the numerical model to try to account for possible mountain-block recharge.

The steady-state model, through its calibration, showed good agreement between observed and modeled groundwater levels from 33 wells. It shows that rainfall diffuse recharge is not enough as input to the system, and additional recharge was needed for the model to run and produce better calibration results (<10% RMS). Transient modeling, considering current estimations of pumping and recharge, shows a negative water balance, with decreasing water levels and an increase in the risk of seawater intrusion. Future potential scenarios of increased pumping and variable recharge show that the system is at risk of a negative water balance, which is especially sensitive to recharge.

The results allow us to suggest future work for monitoring, conceptual understanding and modelling. We recommend a monitoring network of groundwater levels and salinities, abstraction, river discharge, surface-groundwater interactions and climatic variables. The results will allow for better conceptual understanding, especially in terms of the recharge calculations, areas of risk of seawater intrusion and aquifer depletion, and surface-groundwater interactions. Future modeling efforts can include seawater intrusion, contamination, more complex surface-groundwater interactions, a risk of subsidence, and automatic calibration. Without systematic monitoring and regulatory frameworks, groundwater management in Dili will remain highly uncertain and unsustainable.

Finally, this work allows us to suggest the following for sustainable water management: (i) thorough monitoring groundwater, climatic and surface water networks; (ii) regulation policies for pumping and drilling; (iii) measures to increase recharge and minimize flooding (e.g., reforestation of the river catchments, development of infiltration ponds throughout the catchments, prevention of soil impermeabilization and erosion, and structures throughout the rivers to gradually promote infiltration); and (iv) investing in thorough groundwater studies. This is crucial to address knowledge gaps and improve the management framework. The study promotes evidence-based groundwater governance in urban areas where data is scarce, such as Dili City. It also supports the achievement of

several Sustainable Development Goals (SDGs), including SDG 6 (Clean Water and Sanitation), SDG 9 (Industry, Innovation and Infrastructure), and SDG 11 (Sustainable Cities and Communities) [64].

**Author Contributions:** Conceptualization, M.X. and J.A.M.S.P.; methodology, M.X., J.A.M.S.P., and J.M.M.D.A.; software and validation, M.X. and H.G.A.; formal analysis, M.X. and J.A.M.S.P.; investigation, M.X., J.A.M.S.P., and J.M.M.D.A.; resources, I.G.T.L.; data curation, M.X.; writing—original draft preparation, M.X.; review, editing—supervision, J.A.M.S.P., J.M.M.D.A., and F.P.O.O.F. All authors have read and agreed to the published version of the manuscript.

**Funding:** This research was supported by the *Instituto de Geociências de Timor-Leste (IGTL)*, *Timor-Leste*, and conducted as part of a PhD research program at the *University of Coimbra, Portugal*. No external grant number is applicable.

**Data Availability Statement:** The original contribution presented in this study are included in the article. Further inquiries can be directed to the corresponding author.

**Acknowledgments:** This paper is a hydrogeological subchapter of Dili in the first author's Ph.D. thesis written at the University of Coimbra, Portugal, Faculty of Science of the Earth. The authors would like to thank local drilling companies such as H2O Unip. Lda., Mira Mar Unip. Lda., Geotechnical Unip. Lda., and Grupu Fura Bee for sharing drilling data, along with DNMG and DNRAS for climate data. The assistance of the geophysical and hydrogeological teams at IGTL is gratefully acknowledged. The first author also wishes to thank Rifky Meisa Anugrah and Dr. Carlos Miraldo Ordens for their insightful discussions on data analysis. The authors appreciate the anonymous reviewers for their constructive criticism, which has enhanced the quality of this paper.

**Conflicts of Interest:** The authors declare no conflicts of interest.

## References

1. Foster, S.S. The interdependence of groundwater and urbanisation in rapidly developing cities. *Urban Water* **2001**, *3*, 185–192.
2. Omar, P.J.; Gaur, S.; Dikshit, P.K.S. Conceptualization and development of a multi-layered groundwater model under transient conditions. *Applied Water Science* **2021**, *11*, 162. <https://doi.org/10.1007/s13201-021-01485-3>.
3. Sinha, A.K. Groundwater modelling—An emerging tool for groundwater resource management. In *Numerical Simulation of Groundwater Flow and Solute Transport*; Elango, L., Ed.; Springer: Dordrecht, The Netherlands, **2005** pp. 23–42.
4. Elshall, A.S.; Arik, A.D.; El-Kadi, A.I.; Pierce, S.; Ye, M.; Burnett, K.M.; Chun, G. Groundwater sustainability: Interactions between science and policy. *Environmental Research Letters* **2020**, *15*, 093004.
5. Ahmadi, A.; Olyaei, M.; Heydari, Z.; Emami, M.; Zeynolabedin, A.; Ghomlaghi, A.; Sadegh, M. Groundwater level modeling with machine learning: A systematic review and meta-analysis. *Water* **2022**, *14*, 949. <https://doi.org/10.3390/w14060949>.
6. Prasad, Y.S.; Rao, Y.R.S. Groundwater flow modelling of a micro-watershed in the upland area of East Godavari District, Andhra Pradesh, India. *Modeling Earth Systems and Environment* **2018**, *4*, 1007–1019.
7. Wali, S.U.; Usman, A.A.; Usman, A.B. Resolving challenges of groundwater flow modelling for improved water resources management: A narrative review. *International Journal of Hydrology* **2024**, *8*, 175–193.
8. Yihdego, Y.; Danis, C.; Paffard, A. 3-D numerical groundwater flow simulation for geological discontinuities in the Unkheltseg Basin, Mongolia. *Environmental Earth Sciences* **2015**, *73*, 4119–4133. <https://doi.org/10.1007/s12665-014-3697-4>.
9. Anderson, M. P.; Woessner W. W.; Hunt, R. J. Applied groundwater modeling: simulation of flow and advective transport. *Academic press* **2015**, <https://doi.org/10.1016/B978-0-08-091638-5.00015-8>

10. Lekula, M.; Lubczynski, M.W.; Shemang, E.M. Hydrogeological conceptual model of large and complex sedimentary aquifer systems: Central Kalahari Basin. *Physics and Chemistry of the Earth* **2018**, *106*, 47–62.
11. Robins, N.S.; Rutter, H.K.; Dumbleton, S.; Peach, D.W. The role of 3D visualization as an analytical tool preparatory to numerical modelling. *Journal of Hydrology* **2005**, *301*, 287–295.
12. Maxey, G.B. Hydrostratigraphic units. *Journal of hydrology* *2*, no. 2 **1964**, 124–129. [https://doi.org/10.1016/0022-1694\(64\)90023-X](https://doi.org/10.1016/0022-1694(64)90023-X)
13. Seaber, P. R. Hydrostratigraphic units. **1988**, <https://doi.org/10.1130/dnag-gna-o2.9>
14. Wu, J.; Zeng, X. Review of the uncertainty analysis of groundwater numerical simulation. *Chinese Science Bulletin* **2013**, *58*, 3044–3052.
15. Bredehoeft, J. The conceptualization model problem—surprise. *Hydrogeology Journal* **2005**, *13*, 37–46.
16. Abdelhalim, A.; Sefelnasr, A.; Ismail, E. Numerical modeling technique for groundwater management in Samalut City, Minia Governorate, Egypt. *Arabian Journal of Geosciences* **2019**, *12*, 124.
17. Government of Timor-Leste. Pre-Feasibility Study of the Groundwater Resource Development Project for the Water Supply of Dili Metropolitan Area: Draft Final Report. *Team Consulting Group Ltd.; ATT Consultants Company Ltd.; CQ2 Engineering Consultancy Unipessoal Ltd.*: Dili, Timor-Leste, **2020**.
18. Cooper, Yusen Ley, and Tim Munday. "Electromagnetic methods used for the characterisation of aquifers in Timor-Leste." *ASEG Extended Abstracts 2012*, no. 1 (2012): 1–4. <https://doi.org/10.1071/ASEG2012ab409>
19. Wallace, L.; Sundaram, B.; Ross, S.; Brodie, M.S.; Dawson, S.; Jaycock, J.; Stewart, G.; Furness, L. *Vulnerability Assessment of Climate Change Impacts on Groundwater Resources in Timor-Leste*; Australian Government Department of Climate Change and Energy Efficiency: Canberra, Australia, 2012.
20. Pinto, D.; Shrestha, S. Groundwater environment in Dili, Timor-Leste. In *Groundwater Environment in Asian Cities*; Shrestha, S., Pandey, V.P., Shivakoti, B.R., Eds.; Elsevier: Amsterdam, The Netherlands **2016**, pp. 263–286. <https://doi.org/10.1016/B978-0-12-803166-7.00012-X>.
21. Pinto, D.; Shrestha, S.; Babel, M.S.; Ninsawat, S. Delineation of groundwater potential zones in the Comoro Watershed, Timor-Leste using GIS, remote sensing, and analytic hierarchy process. *Applied Water Science* **2017**, *7*, 503–519. <https://doi.org/10.1007/s13201-015-0270-6>.
22. Pinto, D.; Shrestha, S.; Babel, M.S.; Pandey, V.P. Assessment of groundwater yield of the Dili Aquifer, Timor-Leste. *Proc. 5th IPG Int. Conf. on Geoscience Data and Information*, Dili, Timor-Leste, 15–18 November 2022.
23. Ximenes, M.; Duffy, B.; Faria, M.J.; Neely, K. Initial observations of water quality indicators in the unconfined shallow aquifer in Dili City, Timor-Leste: Suggestions for its management. *Environmental Earth Sciences* **2018**, *77*, 711.
24. da Costa, Z.X.; Boogaard, F.C.; Ferreira, V.; Tamura, S. Wastewater management strategy for resilient cities: Case study of Timor-Leste. *Land* **2024**, *13*, 799.
25. Ximenes, M.; Pratas, J.A.M.S.; Azevedo, J.M.M.D.; Figueiredo, F.P.; Currell, M. Identification of hydrochemical processes and assessment of groundwater quality: A case study of the intergranular aquifer in Dili City, Timor-Leste. *Geology, Ecology, and Landscapes* **2025**, *9*, 1–23.
26. Ximenes, M.; Pratas, J.A.M.S.; Azevedo, J.M.M.D.; Ribeiro, J. Evaluating the concentration, distribution, and contamination of toxic metals in the urban soil of Dili, Timor-Leste. *Geology, Ecology, and Landscapes* **2025**, 1–22. <https://doi.org/10.1080/24749508.2025.2535080>.
27. Ximenes, M.; Pratas, J.A.M.S.; Azevedo, J.M.M.D.; Figueiredo, F.P.; Dinis, A. H. D. M. P. Geology of The Lower Comoro Fluvio-Deltaic Accumulation: Outcrop, Resistivity, Drilling Data and Their Implications for Groundwater Resources (under review).

28. Ximenes, M.; Pratas, J.A.M.S.; Azevedo, J.M.M.D.; Figueiredo, F.P.; Currell, M. Assessment of Groundwater Vulnerability in Dili City, Ti-mor-Leste Using an Improved DRASTIC and Analytic Hierarchy Process (AHP) Method: Implications for Wastewater Management (under review)
29. Krohelski, J.T.; Bradbury, K.R.; Hunt, R.J.; Swanson, S.K. Numerical simulation of groundwater flow in Dane County, Wisconsin. *Wisconsin Geological and Natural History Survey Bulletin* **2000**, *98*.
30. Chepkemoi, A. *Evaluation of the Potential of Kericho Aquifer as a Source of Groundwater; Doctoral Dissertation*, JKUAT-CoETEC, Kenya, 2024.
31. Timor-Leste National Institute of Statistics. *Timor-Leste Population and Housing Census 2022: Main Report*; Dili, Timor-Leste, 2023.
32. World Bank. *Climate Change Knowledge Portal: Timor-Leste*. Available online: <https://climateknowledgeportal.worldbank.org/country/timor-leste> (accessed on 20 July 2024).
33. Bogger, S.D.; Spelbrink, L.; Lee, R.; Sandiford, M. Dili 1:50,000 Geological Map. *The University of Melbourne*: Melbourne, Australia, 2013.
34. Instituto do Petróleo e Geologia (IPG). *Geology of Dili Quadrangle and Surrounding Area*; Project Publication; IPG: Dili, Timor-Leste, 2014.
35. Gleeson, T.; Richter, B. How much groundwater can we pump and protect environmental flows through time? Presumptive standards for conjunctive management of aquifers and rivers. *River Research and Applications* **2018**, *34*, 83–92. <https://doi.org/10.1002/rra.3185>.
36. IGTL. Initial Study of Soil Chemistry in Dili City. *Instituto de Geociências de Timor-Leste*: Dili, Timor-Leste, 2023 (unpublished report).
37. Francés, A.P.; Lubczynski, M.W.; Roy, J.; Santos, F.A.M.; Ardekani, M.R.M. Hydrogeophysics and remote sensing for the design of hydrogeological conceptual models in hard rocks–Sardón catchment (Spain). *Journal of Applied Geophysics* **2014**, *110*, 63–81. <https://doi.org/10.1016/j.jappgeo.2014.08.015>
38. Åberg, S.C.; Åberg, A.K.; Korkka-Niemi, K. Three-dimensional hydrostratigraphy and groundwater flow models in complex Quaternary deposits and weathered/fractured bedrock: Assessing increasing model complexity. *Hydrogeology Journal*, **2021**; *29*, 1043–1074.
39. Bhandari, R.; Pathak, D. Groundwater flow modeling in Chitwan Dun Valley (between Narayani River and Lothar Khola), Nepal. *Journal of Institute of Science and Technology* **2019**, *24*, 30–38.
40. Hunt, R.J.; Saad, D.A.; Chapel, D.M. *Numerical Simulation of Ground-Water Flow in La Crosse County, Wisconsin, and into Nearby Pools of the Mississippi River*. U.S. Geological Survey Scientific Investigations Report 03-4154; USGS: Reston, VA, USA, 2003.
41. Barnett, L.; Townley, V.; Post, V.; Evans, R.; Hunt, L.; Peeters, S.; Richardson, S.; Werner, A.; Knapton, A.; Boronkay, A. *Australian Groundwater Modelling Guidelines*. National Water Commission: Canberra, Australia, 2012; Waterlines Report Series No. 82.
42. Prabhakar, M.; Sasikala, D. Groundwater flow modelling using Visual MODFLOW Flex: A case study of the Thuthapuzha Sub-Basin, Kerala, India. *Earth and Space Science Open Archive* **2022**, <https://doi.org/10.1002/essoar.10510217.1>.
43. Harbaugh, A.W. *MODFLOW-2005: The U.S. Geological Survey Modular Groundwater Model—The Ground-Water Flow Process*. U.S. Geological Survey: Reston, VA, USA, 2005.
44. Tamma Rao, G.; Gurunadha Rao, V.V.S.; Surinaidu, L.; Mahesh, J.; Padalu, G. Application of numerical modeling for groundwater flow and contaminant transport analysis in the basaltic terrain of Bagalkot, India. *Arabian Journal of Geosciences* **2013**, *6*, 1819–1833.

45. Chen, Z.; Huang, J.; Zhan, H.; Wang, J.; Dou, Z.; Zhang, C.; Fu, Y. Optimization schemes for deep foundation pit dewatering under complicated hydrogeological conditions using MODFLOW-USG. *Engineering Geology* **2022**, *303*, 106653.
46. Freeze, R.A.; Cherry, J.A. *Groundwater*. Prentice-Hall: Englewood Cliffs, NJ, USA, 1979.
47. Domenico, P.A.; Schwartz, F.W. *Physical and Chemical Hydrogeology*. John Wiley & Sons: New York, NY, USA, 1990.
48. Todd, D.K.; Mays, L.W. *Groundwater Hydrology*, 3rd ed. John Wiley & Sons: Hoboken, NJ, USA, 2005.
49. Hariharan, V., and M. Uma Shankar. "A review of visual MODFLOW applications in groundwater modelling." In *IOP Conference Series: Materials Science and Engineering*, vol. 263, no. 3, p. 032025. IOP Publishing, 2017. doi:10.1088/1757-899X/263/3/032025.
50. Singh, M.K.; Ghosh, S. Groundwater flow modeling for Cachar, India using MODFLOW: A case study. *ISH Journal of Hydraulic Engineering* **2022**, *28*, 232–242. <https://doi.org/10.1080/09715010.2020.1868357>
51. Miall, A.D. *The Geology of Fluvial Deposits: Sedimentary Facies, Basin Analysis, and Petroleum Geology*. Springer: Berlin, Germany, 1996.
52. Healy, R.W. *Estimating Groundwater Recharge*. Cambridge University Press: Cambridge, UK, 2010.
53. Cook, P.; Brunner, P. *Quantification of Groundwater Recharge. The Groundwater Project*: Guelph, ON, Canada, 2025. <https://doi.org/10.62592/BAUS7081>.
54. Adhikari, R.K.; Yilmaz, A.G.; Mainali, B.; Dyson, P.; Imteaz, M.A. Methods of groundwater recharge estimation under climate change: A review. *Sustainability* **2022**, *14*, 15619. <https://doi.org/10.3390/su142315619>.
55. Gun, J.V.D. *Large Aquifer Systems around the World. The Groundwater Project*: Guelph, ON, Canada, 2022. <https://doi.org/10.21083/978-1-77470-020-4>.
56. Ordens, C.M.; Werner, A.D.; Post, V.E.; Hutson, J.L.; Simmons, C.T.; Irvine, B.M. Groundwater recharge to a sedimentary aquifer in the topographically closed Uley South Basin, South Australia. *Hydrogeology Journal* **2012**, *20*, 61–72. <https://doi.org/10.1007/s10040-011-0794-2>.
57. Turc, L. Le bilan d'eau des sols: Relations entre les précipitation, l'évaporation et l'écoulement. *Ann. Agron.* 1954, *5*, 491–596.
58. Putra, D.P.E.; Iqbal, M.; Hendrayana, H.; Putranto, T.T. Assessment of optimum yield of groundwater withdrawal in Yogyakarta City, Indonesia. *Journal of Applied Geology* **2013**, *5*.
59. Rianda, A.A.S.; Putra, D.P.E.; Wilopo, W. Groundwater flow modeling at Sejong Watershed, Sumbawa, West Nusa Tenggara, Indonesia. *Journal of Applied Geology* **2019**, *4*, 43–57. <https://doi.org/10.22146/jag.5320>.
60. Harbaugh, A.W.; Banta, E.R.; Hill, M.C.; McDonald, M.G. *MODFLOW-2000: U.S. Geological Survey Modular Ground-Water Model—User Guide to Modularization Concepts and the Ground-Water Flow Process*. U.S. Geological Survey: Reston, VA, USA, 2000.
61. Pathak, D. R.; Hiratsuka, A. An integrated GIS based fuzzy pattern recognition model to compute groundwater vulnerability index for decision making. *Journal of Hydro-environment Research* *5*, no. 1 **2011**, 63-77. <https://doi.org/10.1016/j.jher.2009.10.015>
62. Alam, F.; Umar, R. Groundwater flow modelling of Hindon–Yamuna interfluvial region, western Uttar Pradesh. *Journal of the Geological Society of India* **2013**, *82*, 80–90. <https://doi.org/10.1007/s12594-013-0113-8>.
63. Inocencio, A.B.; Padilla, J.E.; Javier, E.P. *Determination of Basic Household Water Requirements (Revised)*; PIDS Discussion Paper Series No. 1999-02; Philippine Institute for Development Studies: Makati, Philippines, 1999.
64. Küfeoğlu, Sinan. "SDG-11: Sustainable cities and communities." *Emerging technologies: Value creation for sustainable development*. Cham: Springer International Publishing, 2022. 385-408. [https://doi.org/10.1007/978-3-031-07127-0\\_13](https://doi.org/10.1007/978-3-031-07127-0_13)

**Disclaimer/Publisher's Note:** The statements, opinions and data contained in all publications are solely those of the individual author(s) and contributor(s), and not of MDPI and/or the editor(s). MDPI and/or the editors disclaim all responsibility for any injury to people or property resulting from any ideas, methods, instructions or products referred to in the content.